BRNO UNIVERSITY OF TECHNOLOGY
VYSOKÉ UČENÍ TECHNICKÉ V BRNĚ

FACULTY OF INFORMATION TECHNOLOGY
FAKULTA INFORMAČNÍCH TECHNOLOGIÍ

DEPARTMENT OF INTELLIGENT SYSTEMS
ÚSTAV INTELIGENTNÍCH SYSTÉMŮ

INDOOR DETECTION OF PEOPLE BASED ON VITAL SIGN SENSING

DETEKCE OSOB NA ZÁKLADĚ SNÍMÁNÍ VITÁLNÍCH FUNKCÍ

BACHELOR'S THESIS
BAKALÁŘSKÁ PRÁCE

AUTHOR **DAN PLAČEK**
AUTOR PRÁCE

SUPERVISOR **prof. Ing., Dipl.-Ing. MARTIN DRAHANSKÝ, Ph.D.**
VEDOUCÍ PRÁCE

BRNO 2020

Brno University of Technology
Faculty of Information Technology

Department of Intelligent Systems (DITS) Academic year 2019/2020

Bachelor's Thesis Specification

Student: **Plaček Dan**
Programme: Information Technology
Title: **Indoor Detection of People Based on Vital Sign Sensing**
Category: Embedded Systems

Assignment:

1. Study the literature oriented on vital sign radars and non-contact detection of humans via vital sign. Familiarize yourself with the radars provided at FIT BUT.
2. Propose an algorithmic approach for indoor detection of people based on vital sign sensing.
3. Implement the proposed solution from the previous point. Verify the functionality in real situations.
4. Summarize the achieved results and suggest future direction of the work.

Recommended literature:

- Adib F., Mao H., Kabelac Z., Katabi D. and Miller R. C. Smart homes that monitor breathing and heart rate. In: *CHI '15: Proceedings of the 33rd Annual ACM Conference on Human Factors in Computing Systems*. New York, NY, USA: ACM, 2015, p. 837-846. doi: 10.1145/2702123.2702200. ISBN 978-1-4503-3145-6.
- Aardal O. *Radar monitoring of heartbeats and respiration*. Oslo, 2013. Dissertation. Faculty of Mathematics and Natural Sciences, University of Oslo. Available at: https://www.duo.uio.no/bitstream/handle/10852/37466/dravhandling-aardal.pdf?sequence=1&isAllowed=y.
- Wang G., Gu C., Inoue T. and Li C. A hybrid FMCW-interferometry radar for indoor precise positioning and versatile life activity monitoring. *IEEE Transactions on Microwave Theory and Techniques*. 2014, vol. 62, no. 11, p. 2812-2822. doi: 10.1109/TMTT.2014.2358572. ISSN 1557-9670.

Requirements for the first semester:

- Items 1 a 2.

Detailed formal requirements can be found at https://www.fit.vut.cz/study/theses/

Supervisor: **Drahanský Martin, prof. Ing., Dipl.-Ing., Ph.D.**
Head of Department: Hanáček Petr, doc. Dr. Ing.
Beginning of work: November 1, 2019
Submission deadline: July 31, 2020
Approval date: October 31, 2019

Abstract

Nowadays, in the era of smart solutions and a huge emphasis on data privacy, it is very desirable to detect the human presence anonymously and to recognize if the sensed person is in good health condition. This bachelor thesis is dealing with the detection of people based on vital sign sensing, specifically on the heart and respiratory rate sensing, an algorithmic approach is proposed, and the solution is implemented. The data are sensed via UWB pulse radar or FMCW radar, then the signal is processed, and vital signs are extracted. The thesis presents the experimental measurements and their results.

Abstrakt

V dnešní době chytrých domácností a velkého důrazu kladeného na ochranu dat, je žádoucí provádět detekci přítomnosti člověka a také jeho zdravotního stavu anonymně, a to za pomoci jeho vitálních funkcí. Cílem této práce je provést detekci osob na základě jejich vitálních funkcí, konkrétně tepu a dechu. Za tímto účelem je navržen algoritmický přístup a následně je implementováno řešení. Tep a dech je snímán UWB a FMCW radarem, následně jsou získaná data zpracována a zmíněné vitální funkce jsou extrahovány. V práci je také představeno experimentální měření a jeho výsledky.

Keywords

FFT, vital signs, UWB, FMCW, radar, respiratory rate, heart rate

Klíčová slova

FFT, vitální funkce, UWB, FMCW, radar, dechová frekvence, tepová frekvence

Reference

PLAČEK, Dan. *Indoor Detection of People Based on Vital Sign Sensing.* Brno, 2020. Bachelor's thesis. Brno University of Technology, Faculty of Information Technology. Supervisor prof. Ing., Dipl.-Ing. Martin Drahanský, Ph.D.

Rozšířený abstrakt

Úvod

V dnešní době chytrých domácností a velkého důrazu kladeného na ochranu dat, je žádoucí provádět detekci přítomnosti člověka a také jeho zdravotního stavu anonymně, a to například za pomoci jeho vitálních funkcí. Cílem této práce je provést detekci osob na základě jejich vitálních funkcí, konkrétně tepu a dechu.

Výsledkem je algoritmus pro každé zařízení, které je schopno detekovat, zda je v místnosti přítomna osoba. Pokud je osoba přítomna a zároveň se nachází pod vhodným pozorovacím úhlem, pak je možné detekovat její vitální funkce. Řešení je doplněno o jednoduché grafické rozhraní.

Návrh

Zpracování signálu a detekce osoby

U UWB radarem nasnímaných dat je provedena hardwarová dolní konverze (Downconversion) a ve formátu IQ (In-phase and Quadrature) jsou data poslána do zařízení k následnému zpracování. U přijatých dat je redukován šum vytvořený radarovým oscilátorem. U FMCW radaru jsou data příjata přímo v IQ formátu, která jsou dále filtrována. Každý příchozí rámec se odečte od předchozího a z rozdílu těchto rámců je pomocí Rychlé Fourierovy transformace vypočítána vzdálenostní mapa.

Dech a tep jsou charakteristické periodické činnosti lidského organismu, které pravidelně hýbou tělem (výdech a nádech), a tím mění i vzdálenost mezi detekovanou osobou a radarem. Aby mohly být tyto pohyby detekovány, je z koplexního signálu vypočítána fáze, která je přímo závislá na vzdálenosti mezi detekovanou osobou a radarem.

Za účelem zjištění, zda může radar z příchozích dat zjišťovat vitální funkce, je detekováno, zda se v dané místnosti nachází osoba, zda se daná osoba hýbe, nebo je v klidu. Byly navrženy dva způsoby detekce. První pomocí detekce vlastnostních vektorů a druhá pomocí již vypočítané vzdálenostní mapy.

Extrakce dechové a tepové frekvence

Vypočítaná fáze, v celé snímané délce přímo z filtrovaného signálu u metody feature vectors a nebo ze vzdálenostní mapy u metody druhé, je ukládána do rolujicí fronty se zadanou délkou. Každá horizontální osa maticové fronty znázorňuje měnící se fázi v čase, a to pro danou vzdálenost.

Pomocí Rychlé Fourierovi transformace je vypočítáno spektrum dané měnící se fáze v čase, a to pro každou snímanou vzdálenost radaru. Pokud je v daném spektru nalezena nějaká dominantní frekvence, u které je její mocnost x-krát větší něž průměr mocnosti zbytku signálu, pak je tato vzdálenost vybrána pro detekování osoby.

Frekvence s největší mocností reprezentuje dechovou frekvenci, která je vzhledem k pohybu celého hrudníku dominantní. Frekvence s druhou největší mocností reprezentuje tepovou frekvenci.

Zpřesnění vitálních funkcí

Vypočítané vitální funkce získané z předchozího kroku je možné zpřesnit pomocí 4 navržených metod, protože přesnost výsledku z předchozího kroku je závislá na velikosti výpočetní rollující fronty. První metoda zerro-padding zvyšuje počet vzorků signálu a používá se v kombinaci s nějakou další metodou. Další dvě metody přepočítávají délku periody fáze signálu, a to na základě vzdáleností vrcholů amplitůd a nebo protnutí x-ové osy. Poslední metoda zpřesňuje pozici největšího vrcholu pomocí kvadraturní interpolace.

Implementace

Zařízení

K vývoji byly použity tři radary. Dva od společnosti Infineon a jeden od společnosti Xethru. Radar od společnosti Xethru je typu UWB pulzní radar a radary od společnosti Infineon jsou typu FMCW.

Aplikace

Aplikace byla implementována v jazyce Python3.5, z důvodu existující komunikační knihovny od společnosti Xethru a spousty podpůrných knihoven, nejen pro zpracování signálu jako např.: NumPy, Matplotlib, SciPy. Pro radary od společnosti Infineon byla přepsána komunikační knihovna, která je v jazyce C a byla napojena pomocí standardní knihovny ctypes. Výstupní data jsou zobrazována v jednoduché grafické aplikaci, která byla vytvořena v standardní grafické knihovně jazyka Python tkinter. Nastavení radaru probíhá taktéž v této aplikaci. Data z měření je možné ukládat do JSON souboru.

Experimentování

Byly vytvořeny 3 testovací schémata, které mají simulovat skutečné použití této aplikace. V prvních dvou případech se jedná o místnosti různých velikostí, kde se testovaná osoba vždy posadí na konkrétní místo a po nějaké době se přesune na jiné. V posledním testovacím schématu je monitorována osoba ve spánku. Jako referenční hodnoty slouží údaje z hrudního pásu určeného pro snímání tepu a záznam z mikrofonu pro porovnání dechové frekvence, které jsou během testování zobrazeny na obrazovce.

V rámci testování bylo u prvních dvou schémat testováno 5 lidí s pěti opakováními a u třetího schématu byli 4 lidé monitorováni ve spánku.

Závěr

Hlavní cíle práce byly naplněny, kdy byl na univerzitou poskytnutých radarech navržen algoritmus pro detekci osob v místnosti, a to za pomocí vitálních funcí. Implementace dokáže detekovat vzdálenost osoby od radaru, a pokud je osoba v klidu, tak i její vitální funkce. Funkčnost algoritmu byla prokázana testováním, kdy zařízení od společnosti Xethru dosahovalo výrazně přesnějších výsledků.

Indoor Detection of People Based on Vital Sign Sensing

Declaration

Hereby I declare that this bachelor's thesis was prepared as an original author's work under the supervision of Prof. Ing., Dipl.-Ing. Martin Drahansky, Ph.D. a Prof. (FH) Univ.-Doz. Mag. Dr. habil. Guido Kempter. All the relevant information sources, which were used during preparation of this thesis, are properly cited and included in the list of references.

.....
Dan Plaček
July 30, 2020

Acknowledgements

I would like to warmly thanks to prof. Drahanský for the opportunity to work on this amazing research, for his professional, constructive and relax approach and for acquiring the required equipment. Then I would like to thanks to prof. Kempter and prof Drahanský for arranging and supervising my thesis during my Erasmus studies in FH Voralberg. My sincere thank you goes also to my family, my girlfriend and my friends who support me during my studies, semester abroad and creating my bachelor thesis.

Contents

Chapter 1

Introduction

Everywhere around us is a broad range of a spectrum of radiation. The radiation is coming from the space, but also everything around us is emitting it, including electronics. Electronics are nowadays indispensable gadgets our society cannot function without. These devices are developing rapidly, and one of the main characteristics of modern electronics are devices which are communicating, working and sensing mostly via radio waves.

Radio waves can be used not only for transmitting data but also for detecting objects by radars. Radars had been used mainly for monitoring airspace or as a speed camera, but with the arrival of new, more accurate, harmless-to-health and more accessible technologies, radars are starting to be used to accurately monitoring space in front of the radars. These modern radars are one of the key technologies which people use in modern security, autonomous and anonymous monitoring systems, e.g. radars in autonomous and security systems in vehicles, detection of liquid levels, burglar alarm systems, monitoring and detection of objects including people [2]. Smart home systems use all these benefits plentifully.

Figure 1.1: Radar from autonomous system in car.

This thesis focuses on the usage of radars in the detection of people based on vital sign sensing, namely via two out of four primary vital signs – respiration rate and pulse. In the approach for detection of people, it is necessary to use advanced radar technologies which have sufficient resolution and can detect static objects, e.g. FMCW radars or pulse radars. The significant advantage of this solution is that in the era of the data protection system, we can receive and achieve very accurate data about humans without processing and collecting any personal information (images of persons). This thesis suggests a possible algorithmic approach for indoor detection of people, including the processing of distance

radar signal. In the second part, the suggested algorithm will be implemented, tested, and the results of the tests will be demonstrated.

This thesis was written as a bachelor thesis within the research group STRaDe under prof. Martin Drahanský in Brno University of Technology Faculty of Information Technology.

Chapter 2

State of the art

For the understanding of radars, their set up and usage of the radars, it is necessary to understand specific fields of study – physics of electromagnetic radiation, how radars work. This section splits into three subsections. First deals with physical aspects of radiation, second focuses on Doppler effect, third contains the types of radars, fourth deals with the detection of people and also focuses on currently used technologies of detection of people and last section briefly describes vital signs.

2.1 Physics of electromagnetic radiation

Electromagnetic radiation is everywhere around us, e.g. visible light, radio waves, infrared (heat), microwaves, x-rays, ultraviolet rays. It is a flow of energy (photons). It is synchronised oscillation of mutually linked electric and magnetic fields - electromagnetic waves. The main characteristics of electromagnetic radiation are *frequency* f and *wavelength* λ. The electromagnetic radiation has almost constant speed of propagation (speed of light) in the air $v = c = 3 \cdot 10^8 m \cdot s^{-1}$.

$$f = \frac{v}{\lambda} = \frac{c}{\lambda} = \frac{3 \cdot 10^8}{\lambda} \tag{2.1}$$

Another characteristic of electromagnetic radiation is the energy of radiation. It depends on the frequency of electromagnetic radiation and the constant of the energy of the photon given by Planck's constant $h = 6,626 \cdot 10^{-34} J \cdot s$.

$$W = h \cdot f \tag{2.2}$$

The wavelength characterises the electromagnetic spectrum by the wavelength. It splits into classes by the wavelength/spectrum.

Band	Frequency f	Wavelenght λ
HF and lower	30 Hz - 30 MHz	10 Mm - 10 m
VHF	30 MHz - 300 MHz	10 m - 1 m
P	300 MHz - 1 GHz	130 cm - 30 cm
L	1 GHz - 2 GHz	30 cm - 15 cm
S	2 GHz - 4 GHz	15 cm - 7.5 cm
C	4 GHz - 8 GHz	7.5 cm - 3.75 cm

X	8 GHz - 12.5 GHz	3.75 cm - 2.4 cm
Ku	12.5 GHz - 18 GHz	2.4 cm - 1.67 cm
K	18 GHz - 26.5 GHz	1.67 cm - 1.13 cm
Ka	26.5 GHz - 40 GHz	1.13 cm - 0.75 cm

Table 2.1: Frequency spectrum IEEE. Source [32].

Electromagnetic waves are efficiently reflecting from objects with a similar or bigger size as the size of the wavelength λ. When the object has a smaller size than the size of the wavelength, it reflects waves with lower energy and they are detected worse. That is why recognition of objects with radars are dependent on the frequency of electromagnetic waves transmitted from a radar.

$$\lambda = \frac{c}{f} \tag{2.3}$$

2.2 Doppler effect

Doppler effect (shift) describes a change of frequency of a wave between two objects, where one object is transmitting frequency and the second object receiving it, and the relative velocity between these two objects is nonzero. When the target is moving to the radar, the reflected frequency will be higher than the transmitted one and when the target is moving out of the radar, the reflected frequency will be lower, than transmitted frequency [29] [21]. Doppler *frequency* f_d[Hz] is

$$f_{\mathrm{d}} = \frac{2 \cdot f_{\mathrm{Tx}} \cdot v}{c} \cdot cos\alpha \tag{2.4}$$

where f_{Tx} is carrier frequency, v is object velocity, c is speed of light and α is angel between beam center and target moving direction. With the transformation of this formale is possible to count $v$elocity of the object

$$v = \frac{c \cdot f_{\mathrm{d}}}{2 \cdot f_{\mathrm{Tx}} \cdot cos\alpha} \tag{2.5}$$

2.3 Radars

In this chapter are explained and described principles of how radars generally work and types of radars, which are used in this thesis.

2.3.1 Basic principles of radars

Radar is an electromagnetic device which detects and locates reflecting objects (e.g. people, planes, vehicles, ships). It radiates energy to the space. The signal travels through the space and reflects off objects, and the radar detects echo signals reflected from objects in space. The reflected signal is evaluated in the radar, and it can detect the object. Also from the comparison of transmitted and received signal the radar can compute the velocity of the object. From the time in which signal travels from the radar to the targeted object and back, we can count the distance between the radar and the object. The *range* R is

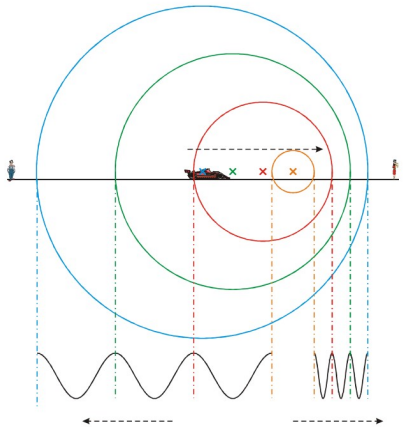

Figure 2.1: Doppler effect. Source: [8].

where c is speed of light, τ is delay of signal (time to object and back).

$$R = \frac{c \cdot \tau}{2} \tag{2.6}$$

The radar composes from these main parts: transmitter, receiver, antenna, evaluation system.

The **transmitter** creates an accurate short duration of high energy frequency and emits it through antennas to space.

The **receiver** receives the echo signal. The received echo signal has to be amplified to an adequate level (depends on the distance of the object) and demodulated.

The **antenna** transfers the transmitter's energy to the signal in space or it can receive any other back. The type, the direction and the settings of the antenna affect the size, the distance and the space of detected objects.

The **evaluation system** compares transmitted and received signals, counts and evaluates data from the signals and detects objects [29] [21].

2.3.2 Types of radars

In this chapter three types of radars are described. Devices used in this thesis can be set as types of radars described bellow. Posetion2Go and Distance2Go can behave as FMCW and CW radar. Xethru X4M03 can be set as Pulse radar.

CW radar

Continuous-wave radar is a type of the radar, where the radar's transmitter transmits a continuous harmonic signal with the constant frequency. The signal reflects off objects and receiver of the radar receives it. When the object is stable (non-moving), the frequency of the received signal is the same as the transmitted signal, and the radar ignores it. When the object is moving, the Doppler effect causes a change of the frequency. The radar compares transmitted and received frequencies, and from the shift of the frequencies, it

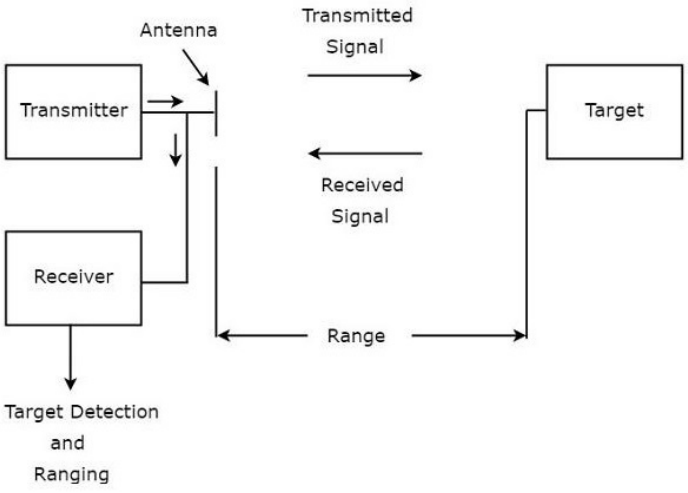

Figure 2.2: Basic principle of radar. Source: [5].

counts the velocity of the object. Because of the continuous harmonic signal with the constant frequency, the radar is not able to determine when the signal is transmitted and when the echo signal is received. Hence the radar cannot count the range between the object and the radar, because the radar does not have the time of the signal's transmission between the radar and the object. FMCW radars deal with this problem [22].

FMCW radar

Frequency modulated continuous wave radar is a type of the radar where a transmitter transmits a signal from the frequency-modulated voltage controlled oscillator. Usually, the modulation is a Sawtooth wave type, because it is easy to ascertain delay of the echo signal. From the frequency modulated signal, the radar can determine (in the mixer) when the signal was transmitted and when it is received. Hence the radar can count the time of transmission between the radar and the object and can count their range. The radar counts the difference between transmitted and received frequencies. From the bandwidth, the period of modulation signal and the difference of the frequencies, the radar counts the distance [15] [29] [22] [19]. Range R between the radar and the object can be counted

$$R = \frac{c \cdot T_{\mathrm{c}} \cdot f_{\mathrm{b}}}{2B} \tag{2.7}$$

where c is speed of light, T_c is up-chirp time, f_b beat frequency, which is corresponding to the target and B bandwidth.

When the object is moving it is necessary to add Doppler shift to the transmitted and received frequencies and then the radar can count the range between the radar and the object as the previous paragraph.

UWB pulse radar

Ultra-wideband impulse radar is a type of the radar, where a transmitter of this radar transmits a short electromagnetic impulse in front of the radar. The impulse is reflecting off the objects and the radar receives the signal through the receiver. For every sample

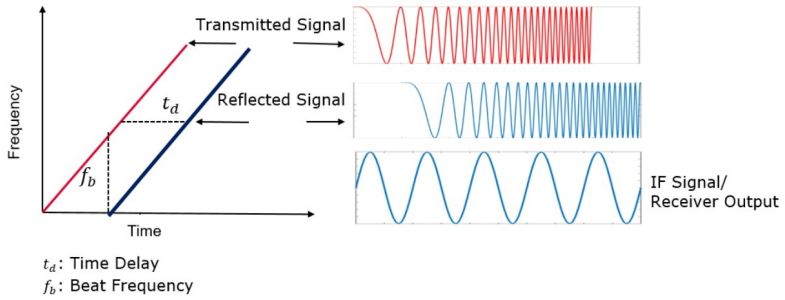

Figure 2.3: Basic principle of FMCW radar operation. Source: [15].

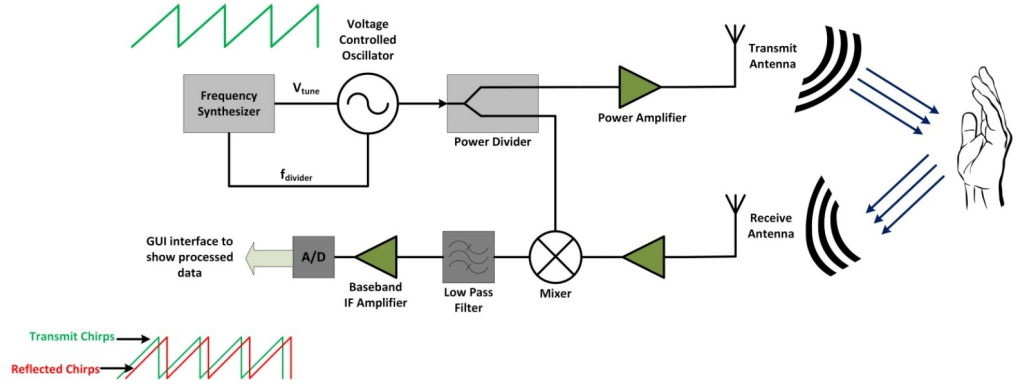

Figure 2.4: Basic principle of FMCW radar. Source: [15].

rate, the radar saves data for each range to the range bin. When the last data of one period is saved , the radar transmits pulse signal again and repeats this process. As the radar sends just an electromagnetic impulse in every working period it radiates less energy than for example FMCW radar (this radar continually transmits the signal). That is why UWB radar can operate with the larger bandwidth and still allow regulations [26].

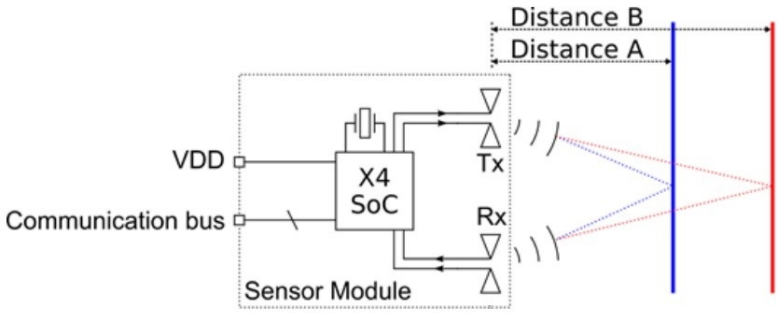

Figure 2.5: Basic principle of FMCW radar. Source: [26].

2.4 State of the art of technologies in the detection of people and their usage

2.4.1 Technologies in the detection of people

This paragraph describes some of the most popular sensors for detecting people.

Radars

Radar is a device, which uses radio waves to ascertain range, velocity, angle and way of movement of objects around the radar. A few years ago, small and relatively cheap microwave radars with good accuracy and reasonable price, appeared on the market. This fact opened new ways how to use them. The radars are now one of the best sensors for the detection of people. They can provide long-range detection (up to 30 meters) in a wide area with high resolution, without daylight, and they can detect more targets. That is why they can be used for measuring speed and distance, monitoring public places, sensing vital signs in smart homes, controling smart homes [2] [33] and also being part of security and autonomous systems.

In comparison with another sensor e.g. PIR sensors, radars with high resolution can recognise humans from animals, and they can detect the direction of movement. Therefore they can also be used for automatic doorway system to reduce their number of openings. When radars detect people via vital signs, they can also detect a state of health of the person and evaluate it.

Radars are usually composed of evaluation and control part, the transmitter, the receiver and the antenna. Their functionality is more deeply described in the Type of radars section.

Digital image recognition

Detection of people is also possible via camera, from video or image. For humans, the visual detection of people is usually an effortless task compared to machines. The problem with this method is the data privacy because of collecting visual data about people. Another problem can be the usage of this method in the adverse visual conditions, but for specific applications thermo-cameras can be used. The camera records the data (image, video) and the it is segmented. It means that objects are separated into specific groups. Further the algorithm extracts features of the groups and from their features and classifies them via a classifier. The classifier can be, e.g. Bayes classifier, K – means classifier or neural network [18].

Lidar

Lidar – light detection and ranging is a sensor for detecting the distance between a sensor and surrounding objects around the sensor via laser. Because of its high accuracy, it is used for scanning surface, including humans and consequent detection of the object (e.g. autonomous systems, tracking people). The sensor has the transmitter, which emits light and the receiver, which is a light sensor and detects the reflected light. From the time of travel of the light, the distance of the object is calculated (from the speed of light). From all distances the sensor creates a depth map of all objects around. These sensors can usually map 2D and 3D space [4].

PIR sensor

PIR sensors are one of the most used sensors for the detection of people. They are mostly in automatic lights or security detection systems and detect infrared radiation (heat). PIR sensor usually composes from two pyroelectric sensors, which are connected as reverse inputs into a differential amplifier. When the sensor is idle, these two parts detect the same amount of infrared radiation (also when the sensor is affected by the temperature changes or sunlight) and signals are cancelled. When the body comes to the detecting area of the sensor, firstly it affects the first pyroelectric sensor and then the second one. This action causes differential change and activates the PIR sensor [13].

Figure 2.6: Light with PIR sensor.

2.4.2 Usage of detection of people

This paragraph describes some of the most popular usages of the detection of people.

Searching people in objects

Emergency services widely use detection of people in or under objects, buildings and in many other places. When members of these services know the exact position of people in the critical situation, they can better assess and analyse the situation and make the right decision. It can also speed up the decision process and save time and lives. Firefighters and rescuers are using detection of people to locate people under avalanches, after earthquakes or in objects under fire [6]. Armed, prison and border services are using it for detection of people before a strike or as an antismuggling human detecting system.

Smart homes and automatic systems

Smart homes and smart electronic usually make their decision based on sensor data, for example temperature, weather, the brightness of light and daylight. When electronics and smart homes can detect people, the system has much more applications. It can smartly track and detect people, turn on/off or regulate light, temperature, open windows or doors and check their vital signs [2] [33]. The system can save energy, lives and enhance the quality of life.

Smart cities

Functions of smart cities are similar to the functions of smart homes. Smart cities use monitoring to run the city more efficiently, for example save money, energy make them

more secure. Trafic management detects pedestrians and vehicles to control traffic lights. Cities also use CCTV with detection of the people to prevent and solve crimes and protect inhabitants against it [9] [32].

Security systems

Security systems are a common part of everyday life. Everywhere around us are private properties and they need to be protected. There are a lot of dangerous and forbidden locations too. These areas and objects can be secured in many ways, but sensors which detect movement or people are used most commonly.

Figure 2.7: Burglar alarm system.

Autonomous safety systems

One of the major characteristic features of autonomous systems are safety features. The highest priority of these systems is to protect people, both direct and indirect users. One of the biggest and most rapidly developing usage of these systems is in transportation, namely in cars, buses, trains and docks. Another, no less important, usage is in factories where big autonomous machines work. These machines have to detect humans when they are around or in their movement trajectory in order to avoid any injuries.

Commercial/statistics purposes

Detecting and tracking of the people is the key activity in stores, transportation and generally in places where is a higher concentration of people. Stores use detection, counting and tracking of the people for marketing purposes. Owners can redistribute selling products to maximise their profits via collected data about where and how long customers are spending their time in the store (data about customers movement). Stores also use collected data to ascertain how many employees they need at the specific time and where (how many cashiers should be open). Carriers use these monitoring techniques in transportation to ascertain how much transport capacity they need.

2.5 Vital signs and their remote detection

2.5.1 Vital signs

The essential physiological functions of the human body are objectively measured by vital signs. Temperature, blood pressure, respiration rate, and heart rate are traditionally con-

sidered as the main vital signs. Abnormalities of vital signs can refer to health difficulties [28]. This work is dealing with the measurement of respiratory and heart rate.

Body temperature

Body temperature is a complex and nonlinear variable. The optimal range varies across living organisms. The temperature of the human body normally ranges from 36.5 to 37.5 degrees centigrade. Several factors can affect the temperature such as diurnal cycles, age, exercise, and menstruation cycle in women [10] [28].

Blood pressure

The blood pressure is the force of the circulating blood on the side of the vas wall. It is a vital sign that reflects the state of homeostasis of an organism . The process of measuring blood pressure consists of gauging systolic and diastolic pressure. The systolic is the maximum pressure felt on the artery during ventricular contractions and diastolic pressure is the pressure immediately before the ventricular contractions occur . The optimal systolic pressure of a healthy person is 120 mm Hg and optimal diastolic pressure is 80 mm Hg . The blood pressure fluctuates during the day and depends on age, gender, state of vigilance of person, on a physical stain, and also mental strain, specifically on weight, emotions, stress, exercise, and also on ethnicity and culture [10] [11] [12].

Respiratory rate

The respiratory rate is expressed by the number of breaths per minute and a normal respiratory rate in an average adult vary around 12 to 20 breaths per minute. Besides its rate also a depth and the pattern of breathing are crucial parameters of the measurement. An increased rate of more than 20 breaths per minute can occur in special conditions such as emotional change, exercise, or pregnancy. Ventilation less than 12 breaths per minute can be related to the consumption of alcohol, narcotics, or metabolic derangements [28].

Heart rate

Recent clinical evidence shows that the normal heart rate in an adult at physical and mental rest range from 50 to 95 beats per minute. However the traditional range used in practice is between 60 to 100 beats per minute. The range varies among gender, specifically, women have a slightly faster rate after puberty. The rate less than 50 beats per minute refers to bradycardia but it can normally occur in the well-trained athlete. Tachycardia is a rapid rate of more than 95 or 100 beats per minute. An increased rate can normally accompany anxiety or exercise [10].

2.5.2 Vital signs remote detection

Radars

There are plenty of approaches to the detection of vital signs via radars which use different techniques and different types of these devices such as CW, FMCW, UWB pulse, Doppler radars. The basic principle of the vital sign detection is based on the changes of the signals, which reflect off the detected target. The changes are caused by the vital signs of breathing and heart rate. A radar's receiver receives the changed signal, then this signal is processed,

and vital signs are extracted. Some of these techniques are also capable to monitor person in longer distances (more than 5 meters) [20].

Visual detection

Nowadays the often used method for the detection of the vital signs is based on the detection of the target temperature via Thermo camera. The heat image of the person is sensed, and then the image is processed and classified, see more detailed description in this section [18].

Another optical monitoring method is based on the photoplethysmogram. This method uses properties of the tissues and the blood when the blood absorbs the light more than the tissues around. This phenomenon changes the optical properties of the skin. The photoplethysmogram is a device which lightens the skin and then the photodetector obtains optical properties of the skin. Based on the properties of the sensed skin, this device is capable of ascertaining the changing main colour components and via signal processing techniques extracts cardiorespiratory [3].

Laser detection

Optical vibrocardiography is another approach to detect vital signs remotely. The laser Doppler vibrometer (LDV) is directed towards the target, usually on the chest of the sensed person. The beam from LDV is reflecting off the chest, and the sensor via Doppler interferometry counts the velocity of the vibration of the surface (chest). This obtained signal is noise reduced, data processed. The frequency from the signal peaks is obtained and also heart rate counted [24].

Chapter 3

System architecture

In the first part, the chapter describes all used sensors in this solution and in the second part proposes a solution for the detection of people based on vital sign sensing.

3.1 Used radars

In this chapter, radars that are used in this research are described.They are three: Infineon Distance2Go development kit [7], Infineon Position2Go development kit [27], Xethru X4M03 [34]. All information about radars are available on the products websites.

3.1.1 Infineon radars

This section describes both radars from Infineon company, which is one of the biggest companies in smart homes embedded solutions. Both radars are FMCW type 2.3.2 and are in this section because they have the same interface, operation and control software. Radars operate in free global available ISM [17] frequency band from 24GHz to 24.25GHz. Kits are optically split into two parts – breakable debugger and sensor board. Radars are built into an evaluation board with Infineon XMC™ ARM® Cortex® - M4 MCU. Their MCU firmware can be redesign and flash into the board via XMC™ flasher on the debugger side of the kit, that is why signal sampling and preprocessing can be performed on the kit. Radars can be connected to the device with micro USB or UART and are distribute with C, Matlab and UART interface and simple radar GUI. The differences between these two sensors are in their hardware specification.

Specification of the Distance2Go development kit

Radar utilises one radar chip transceiver Infineon BGT24MTR11 RF which has one transmitter and one receiver, Infineon XMC4200 32-bit ARM® Cortex® - M4 MCU. The distribution contains four prepared firmwares for this radar for raw, doppler radar, FMCW radar and combination of FMCW and doppler radar data. This radar can generate distance, speed and direction of movement data. See the table below for more specifications 3.1). Price of this kit was 214 USD (2019) [7].

Maximal distance	12 m (human detectable)
Horizontal angel	20°

Vertical angel	42°
Dimension	5 cm x 4,5 cm x 1,2 cm
MCU	XMC4200 32-bit ARM® Cortex® - M4 MCU
Band	24 GHz – 24.25 GHz
EIRP	21 dBm

Table 3.1: Distance2Go development kit specification.

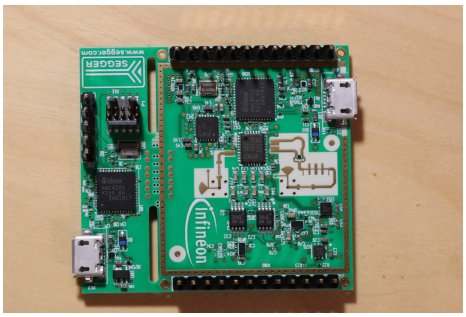

Figure 3.1: Distance2Go development kit.

Specification of the Position2Go development kit

The main difference between the previous and this radar is that this radar utilises one radar chip transceiver Infineon BGT24MTR12 RF which has one transmitter and two receivers, Infineon XMC4700 32-bit ARM® Cortex® - M4 MCU. The distribution contains four prepared firmwares for this radar, for raw, and FMCW radar data. In comparison to Distance2Go, this radar can also generate the angle of an object, thanks to two receivers. See the table below for more specifications 3.2. Price of this kit was 286 USD (2019) [27].

Maximal distance	12 m (human detectable)
Horizontal angel	76°
Vertical angel	19°
Dimension	6 cm x 5 cm x 1.2 cm
MCU	XMC4700 32-bit ARM® Cortex® - M4 MCU
Band	24 GHz – 24.25 GHz
EIRP	18 dBm

Table 3.2: Postion2Go development kit specification.

3.1.2 Xethru radar

The last sensor is from the company Xethru which is focusing on smart homes and presence and respiration sensors. This sensor X4 is UWB pulse-type 2.3.2 and can work on 7.29.

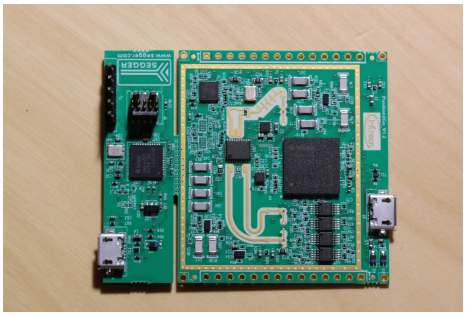

Figure 3.2: Position2Go development kit.

Development kit's name is Xethru X4M03 and consists of three parts: X4SIP02 radar subsystem (with X4 chip), antenna board and XTMCU02 MCU board with ARM® Cortex® - M7 MCU. On the radars kit, setting up, communication, signal sampling, preprocessing and processing can be done via Xethru Embedded Platform. After development it is possible to produce this solution in high volume with single board X4M02. Kit X4M03 because of the low power spectrum, is certified for usage in EU, USA and Canada (CE/ETSI, FCC, ISED). Radar can be connected to the device with USB, UART and GPIO and is distribute with the interface to Matlab, Python, C++ and C.

Specification of the X4M03 development kit

Radar utilises oner radar chip Xethru X4, ARM® Cortex® - M7 MCU. See the table below for more specifications 3.3. Price of this kit was 399 USD (2019)[1].

Maximal distance	10 m
Horizontal angel	65°
Vertical angel	65°
Dimension	5.8 cm x 3 cm x 1.5 cm
MCU	ARM® Cortex® - M7 MCU
Band	7.29 GHz
EIRP	-15.5 dBm

Table 3.3: X4M03 development kit specification.

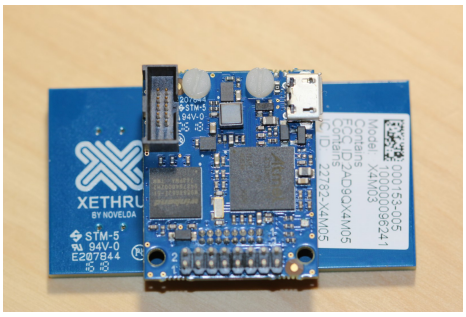

Figure 3.3: X4M03 development kit.

[1]Xethru shop: https://shop.xethru.com/x4m03

3.2 Algorithm description

The detection of people based on remotely vital sign sensing is built on precise detecting of the range between the target and the radar. Human bodies with their breathing and their heart beating change the distance between the body and the radar (inhalation and exhalation) periodically [2], and it creates periodic signals, which are visible in radar's radio frequencies. The radar senses these signals, they are hardware segmented, preprocessed (remove clutter and noise) and because of the discrete periodical respiratory and heart rate signal the FFT (fast Fourier transformation) is used. This algorithmic approach consists of four parts: Signal preprocessing, Detection of human, Respiratory, and heart rate extraction and Vital sign accuracy improvement. The main idea to use FFT for vital sign detection comes from this article [1].

3.2.1 Signal preprocessing

Downconversion

Radar provides a higher raw radio frequency signal. To enhance the provided data, a downconversion method is used. Those data contain less noise and they are converted to lower frequencies with no modulation. This method also preserves the data information. The downconversion converts radio frequency signal into the baseband signal which is usually represented by complex IQ data. In the downconversion, the sampled radio frequency signal is multiplied by complex sine with the frequency, which is equal to the transmitted pulse frequency. After this multiplication, pulse frequencies are centered at sum and difference frequencies. The lowpass filter filters out the sum frequencies and keeps the difference frequencies (filter out band energy). The signal can be downsampled with decimation (holds only Xth sample) [26].

In-phase and Quadrature

Data from the radar are represented by IQ data (In-phase and Quadrature) because analogue/digital converter converts only the real part of the complex signal. To gain a full complex signal it is necessary to angle modulate the second component of the IQ signal, the Q component. It means that the I component contains only the real part of the complex signal and Q component contains "phase quadrature" signal, signal 90° out of phase (i.e. $\pi/2$), the imaginary part of the complex signal. Since cosine is $\pi/2$ shifted compared to the sine, these formulas can be used for definition of IQ components 3.1 3.2.

$$I = A\cos(\phi) \tag{3.1}$$

$$Q = A\sin(\phi) \tag{3.2}$$

From IQ signal it is easily possible to count signal magnitude (amplitude) A 3.3 and phase ϕ 3.4 [23].

$$A^2 = I^2 + Q^2 \tag{3.3}$$

$$\phi = \arctan(\frac{Q}{I}) \tag{3.4}$$

Phase noise reduction

When the radar is sensing unchanging space in the radar's phase of the signal, small random fluctuation differences between each time frame are present. These differences are causing additional noise of the radar signal. The oscillator of the sampling system generates them by its oscillation. This solution is comparing differences between the time frames, and these small vibrations can add the unwanted signal's frequencies, which can harm the future signal processing. That is why it is necessary to remove this noise from the signal. For this reason, the phase noise correction method is used. Firstly the reference bin is selected (signal of the specific distance), where the movement should not be present (one of the first bins) and the reference phase value for this bin is sensed (mean of the last x values of this specific bin). After obtaining the reference value, every other frame is phase corrected. In the phase noise correction, firstly the difference between the reference bin's phase value and the current bin's phase value is counted. This difference shows the phase noise of the specific frame, and to get rid of this noise, phase shift through all bins is needed. Because the phase noise is correlated throughout the frame and the downconverted baseband data are used, the phase shift can be done by the multiplication of the signal frame by the complex factor of the phase difference. The result of the multiplication is phase corrected signal [25].

Direct path

The main principle of the function of radars is transmitting the signal from the transmitter and receiving it with the receiver 2.3.2. When the signal is transmitted, part of the signal goes straight from the transmitter to the receiver. This causes higher reflection (signal) intensity at the begging of the received signal and that is why these bins are ignored.

3.2.2 Detection of human

Detection of the human is based on accurate sensing of a change of the distance between the radar and the person. To get an accurate change of the distance the phase of the signal is counted from the obtained IQ signal 3.4, because the change of the signal's phase in the time depends on the change of the distance in the time and wavelength of the transmitted signal λ 3.5. Wavelength is invariable in time, and that is why the signal's phase depends only on the distance [31].

$$\phi(t) = 2\pi \frac{d(t)}{\lambda}. \tag{3.5}$$

Feature vectors detection

The algorithm counts the signal's phases for all bins (all specific distances) in every sweep, and it saves these phases into the rolling buffer of the size of an evaluation window (sampling frequency * time of the window). The rolling buffer is a matrix buffer which represents changing of the phase in a specific bin in the horizontal time dimension, and in vertical dimension it represents bins. 3.4. To obtain vital signs from the space ,where the target person is located, the person's bin needs to be detected in the evaluation window.

Detection of the person is executed via FFT because phase in the evaluation window is a discrete signal and the vital signs create periodic movements. These movements can be detected in the FFT's output which is in the spectral domain and the absolute value of the FFT's output represents the magnitude of the frequencies from the imputed phase signal.

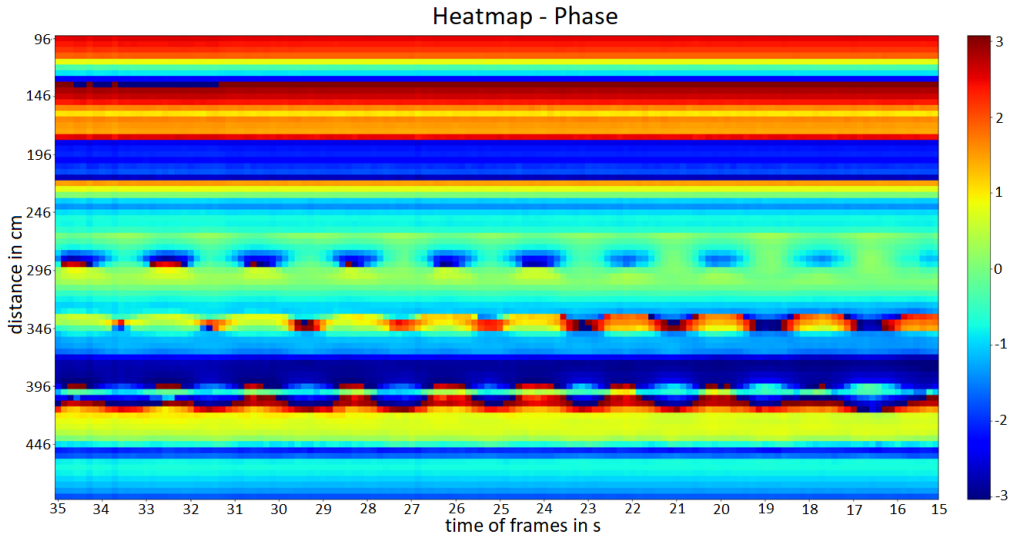

Figure 3.4: Heatmap of the evaluation window.

Because breathing is a dominant periodic signal, localization of the breathing periodicity is performed by the method of the sharpness of its FFT magnitude spectrum.

If the biggest FFT's magnitude peak is x times higher than the arithmetical mean of the remaining magnitudes, then it shows that this signal is strongly periodic and the peak frequency is probably a breath rate. This algorithm takes only the first bin which matches this criterion, because when the signal reflects off the person (or another object), part of the signal can reflect off the target not directly back to the radar, but to the wall. Then it reflects off the wall into the radar indirectly. This phenomenon is called Multipath and creates bins behind the original one, which have similar signal characteristics 3.4.

The signal from the movement of the sensed person can contain more powerful frequencies, and the algorithm can falsely detect this stronger frequency magnitude, which incorrectly substitutes the breath rate. To avoid the false interpretation of these data in the evaluation process, the feature vectors of the specific device's evaluation window are extracted and saved as thresholds. The comparison of the current feature vectors with the saved ones can show if the human is present in the evaluation window, if he is moving or if he is calm. Also the person's vital signs can be detected. As a feature vector are used: an average of the bins maximal peak's magnitude, an average of the bins remain magnitude, an average power of the bins (frequency multiplied by its magnitude).

Fast range detection

The second algorithm for human detection is built on the Fast range algorithm (FFT of all distance bins) [19]. The incoming signal contains static and non-static objects, and the algorithm has to recognize if there is a person, if the person is moving or if it is calm and if it can be measured from the frame (or mean of the chirps in the frame in FMCW radars). The algorithm counts and subtracts every incoming FFT's frame from the previous FFT's frame. This method removes static objects from the frequency spectrum [2]. The result of the subtraction is transformed as the function of the distance in the time and its phase is

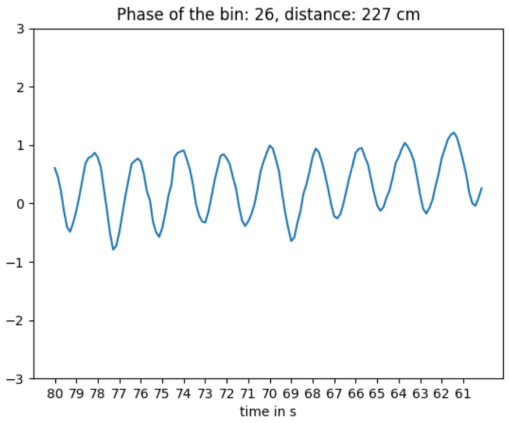

Figure 3.5: Phase variation in time.

saved into the rolling buffer. The algorithm selects as a target the non-static object with the distance, which has the highest absolute result of the multiplication of the imaginary and complex component of the signal in the specific bin 3.6.

$$result = |Re * Im| \tag{3.6}$$

Both methods can usually handle small movements of limbs. While the person is static, the limbs are usually discarded because they are present in different bins. When the limb motions are aperiodic and stronger, they can mask breathing and heart rate in detecting time window. This method works with small movements such as writing on a laptop, checking the phone. These movements are aperiodic, but usually, they do not mask breathing and heart rate and in another step are filtered as white noise.

The respiratory and heart rate signal is periodic compared to other movements. That is why we can detect this signal when the person is not facing the radar. When the person is facing the radar with its back, the signal is vice versa.

In FMCW radars additional methods for extraction of extra data such as angle and speed of a target can be used . Doppler range (slow range) can be computed from the new FFT of the fast range of each chirp. The new FFTs are computed from all chirps of every single bin. The maximal value from FFT magnitude is the correct velocity of the bin, and via multiplication of the maximal wavelength per meter by doppler frequency per each bin, the speed of the target can be computed [19].

If the radar has two antennas, an angle of the target in space can be computed. The algorithm selects the highest value from the slow range's bin of the target from both antennas. Then the algorithm computes the difference of these values, and the target angle is computed from this formula 3.7 [14].

$$target\ angle = \sin^{-1}(\frac{\phi}{2\pi} \times \frac{\lambda}{wave\ lenght\ spacing\ antenna}) \tag{3.7}$$

3.2.3 Respiratory and heart rate extraction

In the previous step the bin was selected, the phase of this bin was obtained and the information, if the data can be used, extracted. If the person is calm and the person's vital

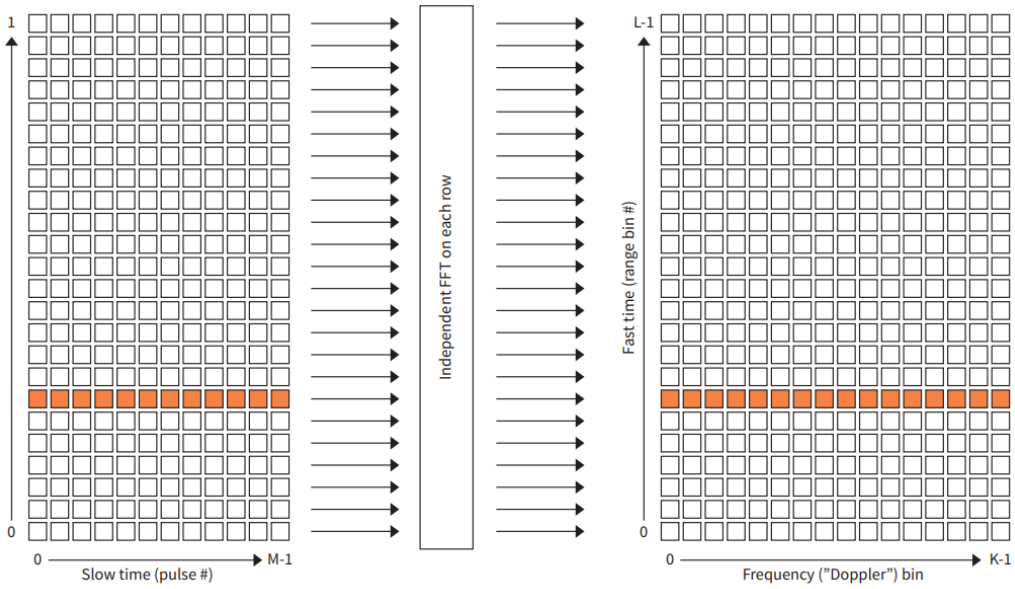

Figure 3.6: Ilustration of counting Doppler (slow) range map. Source: [14].

sign can be monitored then the algorithm continues with the spectral analyses to the next step.

Basic respiratory rate extraction

The estimated respiratory rate is obtained by performing FFT on the selected bin (phase of the reflected signal in time) The maximal peak of the FFT (the most significant spectrum magnitude) gives us an initial estimation of the respiratory rate. The respiratory rate is computed by multiplication frequency of the maximal peak by 60 (frequency is converted to breathe per minute). This method's accuracy is reliant on the accuracy of the FFT spectrum 3.8

$$frequency\ accuracy = \frac{1}{T}, \tag{3.8}$$

where T is the total time of the evaluation window. The evaluation can be provided more frequently than the time of the evaluation window. If the person is motionless after some movement, the strong movement signal persists, and it is not possible to sense the person during the time in which the signal is in the evaluation window.

In the phase-frequency ,the strongest peak can sometimes belongs to the lower frequency which cannot be considered as a breath rate. This signal can be filtered out via allowed frequencies for the respiratory rate (i.e. respiratory rate has to be higher than 3 bpm).

Basic hearth rate extraction

Heart rate signal is a periodical signal modulated on the top of the breath signal. This signal is weaker than the respiratory signal, and it can lead to the problem that the stronger respiratory signal masks the weaker heart signal in the adjacent frequencies. To moderate this problem, the algorithm in FFT frequency spectrum keeps only signals with 40 and

higher frequencies per minute (beats). This filter removes breath frequency (usually 8-16 breaths per minute). The maximum peak's frequency (not the maximum value) of the filtered FFT spectrum should represent approximate heart rate frequency with the accuracy as in the breath rate 3.8. The heart frequency needs to be converted to minutes as in breath rate.

3.2.4 Vital sign accuracy improvement

The initial vital sign value's accuracy can be improved with additional spectral methods. Zero padding has to be applied before the FFT, and the other methods have to be used after the basic vital sign extraction. Zero crossing and Detection of Amplitude peaks methods are used for detection of the period of the given signal. The quadratic interpolation method counts the peak more accurately than the given peak and Zero padding method improves the number of samples in the spectrum.

Zero padding

Application of the zero padding method can be applied together with one of the mentioned methods bellow because they start after computation of FFT. On the contrary, the zero padding starts before the computation of the FFT. Zero padding method has two main advantages. It adds zeros to the end of the signal. Because of that, the FFT input signal is more extended, and that is why the FFT result represents a longer vector which contains more samples in the output FFT frequency spectrum. After the zero padding computation, the resulted spectrum has more samples and is more smooth, but the main information such as the position of the peak is unchanged. The second advantage of this method is that the Fast Fourier Transformation algorithm works more efficiently with the input signal's total length which is N power of 2. That is the reason, why zero padding can be used to pad samples to achieve the signal's total length N power of 2.

The new frequency of samples has to be recomputed after application of the zero padding via the formula below.

Zero crossing

Zero crossing method works with a signal which contains only the hearth/respiratory signal. In the previous step 3.2.3, the algorithm found the frequency spectrum peak of the hearth/respiratory signal. This method keeps only the peak, and both adjacent values and via inverse FFT (IFFT) computes the complex time-domain signal, which describes only the hearth/respiratory signs. This method keeps the adjacent values because they can contain part of the main (peak) signal. Since the inversed signal does not have an optimal resolution to find the zero-crossing points precisely, the cubic spline is used for computation of more points.

In the next step in this inversed and interpolated signal, the zero crossings are found and the distances between them are computed. To get the length of the period from the total distance, the average distance between two zero crossings is counted and multiplied by 2. Length of the period represents the time of the period of the imputed inversed signal, which is the phase of the bin's signal in time. In the final step the number of period in one minute is counted (60 divided with the period of the signal).

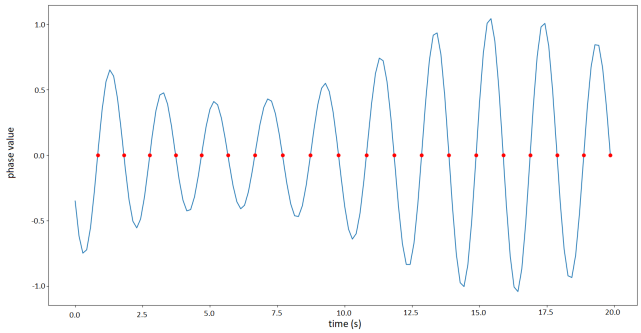

Figure 3.7: Zero crossing method with crossing points.

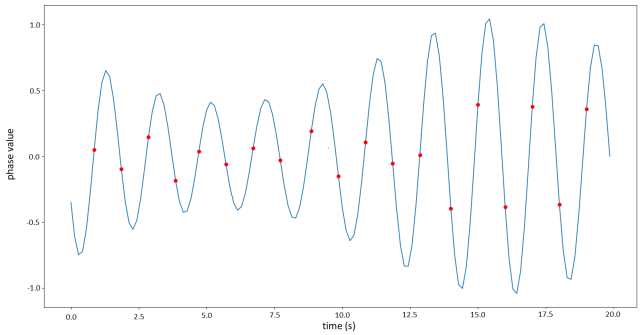

Figure 3.8: Zero crossing method without cubic spline with crossing points.

Detection of Amplitude peaks

Detection of Amplitude peaks works on a similar principle as zero crossings. In the first step, the inverse signal is obtained as in the Zero crossing method. This method does not need any spline improvement step.

The different part of the method compared to zero crossing is in the section where the distances between points are counted. The distances are not between zero points but between the peaks of the amplitudes (local maxima). The rest of the algorithm has the same steps as zero crossing. Thus the average length between the peaks is counted and the period is converted to the minute rate.

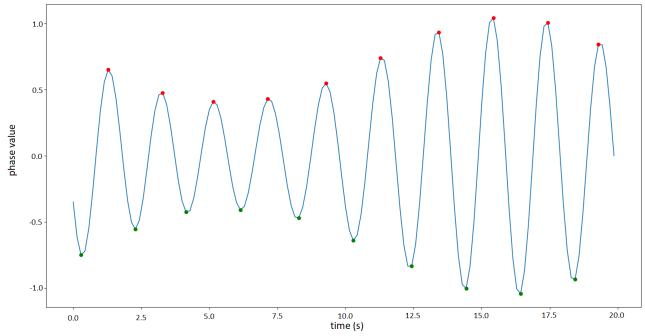

Figure 3.9: Detection of amplitudes method.

Quadratic interpolation

The quadratic interpolation can be used to compute more accurately the peak of any sinusoidal signal. The signal spectral's peak is usually substituted with polynomial or parabola, and it is counted from the original peak and its adjacent values. This new peak should become more accurate. This formula is counted from parabole [30] and variables are described in the scheme.

$$p = \frac{1}{2}\frac{\alpha - \gamma}{\alpha - 2\beta + \gamma} \tag{3.9}$$

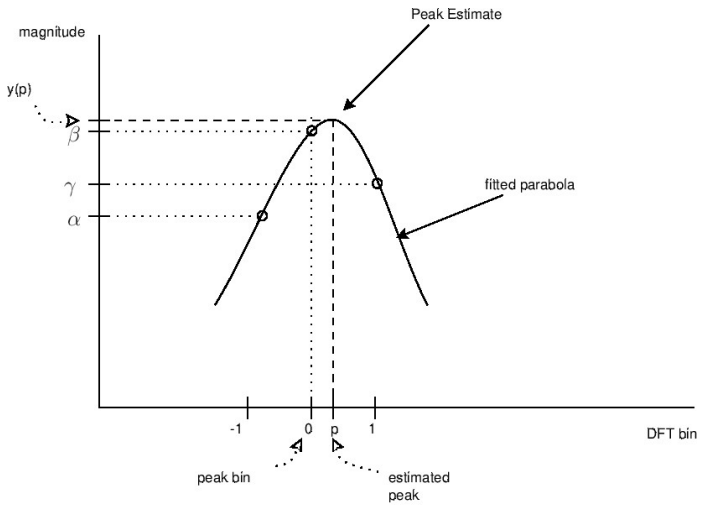

Figure 3.10: Quadratic interpolation method. Source: [30].

Chapter 4

Realization and experiments

In this chapter, the realization of the proposed solution, explanation of the final choosen methods, decisions which were made, ultimate experiments and evaluation of the solution are described.

4.1 Realization

This section describes the installation and implementation of the proposed solution in Python programming language. Specifically, how the radars behave in specific situations and why particular methods were chosen or refused.

Tools installation

The solution is proposed, implemented and tested in programming language Python 3.5 because communication library for radar Xethru X4M03 is provided only in the version for Python 3.5. The Python 3.5 needs to be installed according to the operating system. The solution requires these installed Python libraries: Scipy and Numpy for mathematical computations, Matplotlib for printing graphs, Pyusb for ascertaining all connected USB devices, Pyserial and Configobj for Xethru module connector. Libraries are available in pip package-management software.

```
$> pip3.5 install package-name
```

Figure 4.1: Installation of the package.

Xethru provides a module connector library in the version for Matlab, Python and C++ language for Unix and Windows operating systems and is available here[1]. The module connector in folder "ModuleConnector-Unix-135-x86$_6$4 − *Linux* − *gnujhastobeinstalled*.

Company Infineon provides a communication library for each radar in versions for Matlab and C language for Windows and Unix operating systems. They offer another communication library for its platform, which already contains some preprogrammed processing solutions. It is in C language, it can be adjusted and run only on their DAVE project platform. To the DAVE project, it is necessary to flash the correct firmware via XMC™

[1]ModuleConnector: https://github.com/novelda/Legacy-SW/tree/master/ModuleConnector

```
$> python3.5 setup.py install
```

Figure 4.2: Installation of the module connector.

Flasher. This solution uses only basic communication libraries, that is why no flashing is needed. All software from the Infineon is available in the Infineon's program "Infineon Toolbox" [2].

Implementation

The solution is programmed in Python 3.5. There are 3 versions of the solution, for each radar one version, and these solutions are similar. Each version is suited for the specific radar, e.g. setting up the radar's parameters and features specific for the particular radar and obtaining different pieces of information. The versions among FMCW radars are more alike than the UWB radar version because they contain the same communication library and they are working on the same principle. The only differences are the usage of different settings and filters and that they are obtaining different pieces of information.

Communication library and setting up radar

Infineon radars
Connection of Infineon's communication library with radar is provided with C communication library. This library contains 9 modules and each module sets up and obtains different settings and data. Because functions in the communication library distribute data via callback functions, these functions were rewritten to return these values, not to the callback functions but to be returned as return values. The rewritten functions were added to the original modules and their names differ from the original ones in the ending *_Python*. All modules were compiled with created Makefile, which creates a shared library with the name *communLib.so*. *CommunLib.so* is connected with Python via ctypes standard Python's library [3]. In Python's modules C Communication library's structures are created, and the shared library is connected to the solution.

```
1 SharedLib = ctypes.CDLL(str(libnameOfDevice))
```

Figure 4.3: Connecting C shared library into the Python program.

In the *main.py* file, the Infineon device is searched in the port list and connected via functions from the communication library. For each communication library which is used in the solution, the library endpoint is created. If the device is found, the initialization (in desktop type it is executed in *desktop.py* file) and specific type of program are executed such as desktop application, real-time heatmap application and real-time raw data plot application. In *initialize.py* the radar's settings are set up. Main settings are number of samples per chirp, number of chirps per frame, the format of the received signal, FIFO buffer, scanning period, etc.

[2] Infineon toolbox: https://www.infineon.com/cms/en/tools/landing/infineontoolbox.html
[3] Ctypes library: https://docs.python.org/3.5/library/ctypes.html

Xethru radar
Xethru radar is provided with a Python library and after the installation from the previous chapter can be immediately imported to the project.

```
1 from pymoduleconnector import ModuleConnector
```

Figure 4.4: Importing module connector into the program.

In the *main.py* the Xethru device is searched in the list of ports via Python's library pySerial. If the device is found, the specific type of application is called (desktop application, real-time heatmap application, real-time raw data application). The initialization of the radar takes place after selection of the type of the program. The initialization is in the file *initialize.py*, where the radar is connected, and new settings are updated. The settings are DAC level, scanning frequency, enabling downconversion, pulse per step, offset and sensing distance. In this file, the phase correction's reference value is also computed.

Control of the algorithm

The main control functions are placed in the *control.py* file, and they are called from the main or a graphical module. The functions are similar for both radars because the principles of final algorithms are almost the same.

The first helping function is *emptyBuffer*, which empties FIFO radar's buffer before vital sensing. The first main function is *realTimePlotData* which provides real-time plotting of the magnitude of the complex signal and the phase of the complex signal in the solution for Xethru radar. In the solution for Infineon radars, this function provides real-time plotting of the fast and the slow range of these radars and prints the distance and speed of the detected target. In the Position2GO it prints angel of the target too.

The rest of the main functions, which are called *plotHeatMap* and *localizePerson*, provides the detection of the person based on vital signs sensing and the values of the vital signs of the target. The function *plotHeatMap* has an initialization and settings at the beginning of the application, and after the initialization, the localization algorithm begins running in the infinite loop. This function can optionally plot the heatmap of the evaluation window, phase of the selected bin and FFT magnitude of this bin.

The function *localizePerson* is repeatedly called from the GUI module and contains only one cycle of the algorithm. That is why the initialization is called from the GUI before the first cycle of this function. The initialization is placed in the second helping function *initLocalization*. Both functions have a similar evaluation cycle. The evaluation cycle obtains and preprocesses new data, and if it is evaluation iteration, it extracts new data from the evaluation frame. No timer for obtaining new data is needed because all radars have FIFO buffer, and they obtain data based on the set time period.

If the printing is enabled, it prints computed data, or if the saving data is enabled, it saves data into the output file. At the beginning of the algorithm, feature vectors are counted, the distance of the target is obtained, and if the target is calm, the evaluation bin is selected. These steps are performed via functions from the *getTarget.py* file. The selected bin's phase can be adjusted with merging of the adjacent frames, filtered with the median filter, which uses only one adjacent value from each side or zero-padded. In the last section, the absolute value of the FFT output is counted, and via different methods, the vital signs are extracted and enhanced from the magnitude. These methods are in the file *getVitalSings.py*.

Data acquisition

Raw data from the radar are obtained and preprocessed in functions which are in file *getData.py*.

Infineon radars
The function *getComplexFFTRangeData* obtains the whole data frame from radar's FIFO buffer and based on the frame pieces of information and radar settings, this function reads the data and saves them as a complex signal. The raw data represents the original frames which are divided into sections, where each section represents one complex component from one antenna with all chirps.

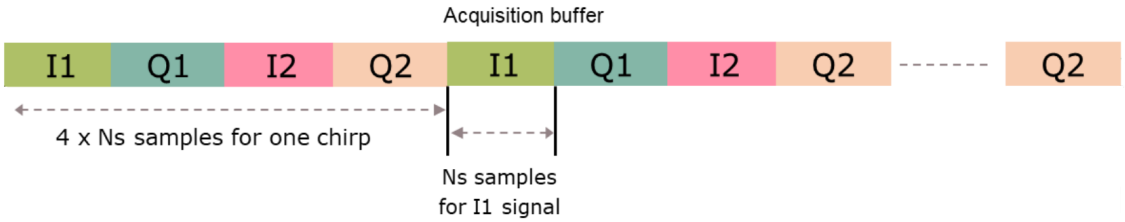

Figure 4.5: Data acquisition. Source:[16].

The file contains the second helping function *emptyRoomFrame* which senses the empty room after the set delay and counts the mean of the empty room's complex signal. These data can be used for subtraction with the new obtained complex values to get only the places where something is changed. This method is not used in the final solution, because it does not bring an improvement, but the algorithm can be turned on in the desktop application.

Xethru radar
There are three functions in the file *getData.py*. First function *readFrame* reads the radar data from the radar s FIFO buffer, and if the downconversion is enabled, this function assigns the first half of the frame as I component and the second half of the frame as a Q component of the complex number. In the next step, this function executes phase noise correction and computes noise corrected phase from the complex signal. The phase noise correction class was programmed by company Xethru, adjusted by the author of this thesis and comes from this article [25].

The downconversion is used because the raw data need to be converted to a lower complex signal without any modulation. The downconversion can be performed by software signal preprocessing, but in this solution, it has no additional advantages, that is why the hardware downconversion is used. Function *realTimeDataProcessing* prepares data for real-time plotting by counting the absolute value of the complex signal.

The last function is *saveData*, and this function manages the rolling buffer. In the first run, it initializes new rolling buffer for values and saves new values into the buffer, in other runs, it rolls the buffer and saves new values.

Localization of the target

Localization functions are placed in the file *getTarget.py*. In all final solutions, the feature vectors method is used because of achieving better results. The method based on the fast

range detection has a problem with the precise detection of the static target. The static target distance was changing up to 0.7 meters, and often the algorithm has a problem to detect the target at all.

That is the reason why the feature method was selected for the final solution. The feature method needs the feature vectors to realize if the selected bin can be used or not. Three feature vectors are used in the final algorithm. The first one is the average of maximal FFT magnitude spectrum's values in all bins and the second one is an average of the remain values in the spectrum in all bins. Both values are computed during the process of selecting the target bin in function *localizeBin*. The last value represents the average FFT magnitude spectrum's power in all bins (value is multiplied by its frequency) and is counted in function *powerFrame*. Other features vectors were tested but no correlation between them and the target's movement status was not founded. There are similar to the used feature vectors, but the averages are not obtained in horizontal but in the vertical dimension. The other feature vector is an average of the difference between the current and one of the previous frame which was obtained. These features can be obtained in the functions *verticalDifferenceFFT* and *verticalAvgFFT*.

The distance of the target based on selected bin can be obtained by all these radars. Since the position2GO radar has two antennas, the angle of the target can be obtained. Infineon's radars signal has a bad resolution where one bin has a resolution 0.75 m, because of that the distance and the angle cannot be precisely determined. The detection of the target was tested in the provided application by Infineon. Their detecting solution shows the incorrect changes of the distance and angle even when the target is static. These radars are more suited for outside detection.

Radars are capable of measuring signal only from the target, which is in the same room. They are not able to obtain a signal behind the door, wall, etc.

As a localization algorithm, the feature vectors detection was selected for both radars because this method obtains data with a better result in all devices. This method is implemented in function *localizeBin*, and it returns the selected bin, and two feature vectors. The bin is selected if the maximal peak value of the FFT spectrum is x times higher than the average value of the remains values. If the bin is selected, the next x bins can be chosen instead of the selected bin in case that they have better signal characteristics than the previously selected bin. The criterion is the difference between the maximal peak value and the average of the remain values. The maximum amount of possible reselected bins is also set in the algorithm.

In Infineon radar's solution, the function *localizeTarget* is called before function *localizeBin*. This function provides localization based on fast range. In the beginning, the mean value of the radar's signal is subtracted from itself, and the Hanning filter is used. The signal has to be zero-padded because the bin's resolution is a 0.75 m. The phase of the zero-padded fast range is saved into the rolling buffer and used in *localizeBin* function. From the slow range, the speed and from position2GO's both antenna's slow range and the angle of the target is computed.

Extracting vital signs

When the bin is selected, the vital signs are extracted from the bin's phase in the evaluation window via functions located in the file *getVitalSings.py*. The function *getMaxPeakFreq* obtains the biggest maximum peak from the given signal, which is bigger than the threshold frequency. In this program, the signal is FFT spectral magnitude. When this function is

called for the next time in the same cycle, then it continues where it stopped in the last call. This function returns only basic vital signs with the accuracy of the FFT magnitude spectrum 3.8.

The rest of the functions in the file *getVitalSings.py* take the results from the function *getMaxPeakFreq* and recompute new result from it. Quadratic interpolation method is implemented in the function *quadraticInterpolation*. Method Detection of amplitude peaks is implemented in the function *peaksOfAmplitudes*. The last function is *zeroPoints* which represents method zero-crossing where the cubic spline is used for better estimation of the zero-crossing points. These zero-crossing points search is based on finding two sequent points with a different sign. The point with the lower absolute value is chosen. All these algorithms are described in the section 3.2.4.

GUI

The graphical user's interface is built via tkinter Python's standard library [4], and it is implemented in the *GUI.py* file. The GUI has 3 main sections: Home page, Settings and Help. In the home page in the left-sidebar are shown all the boxes with pieces of information from running application based on the current settings and button for starting and stopping the application. In the right side of the application is a circular sector with sectors which show where the localized person is in the space. The settings section represents settings of parameters which are used in the application. The help section represents the help page of the application.

The GUI is implemented as a class *Window* which holds the GUI's and the application's data. This class has a couple of methods which control GUI and update application settings. In this file is function *drawMap*, which draws the circular sector's localization map via Python's turtle library. There are 3 other helping functions in this file which help with the starting and the ending of the localization algorithm. *DesktopApplication* function starts and initializes the GUI.

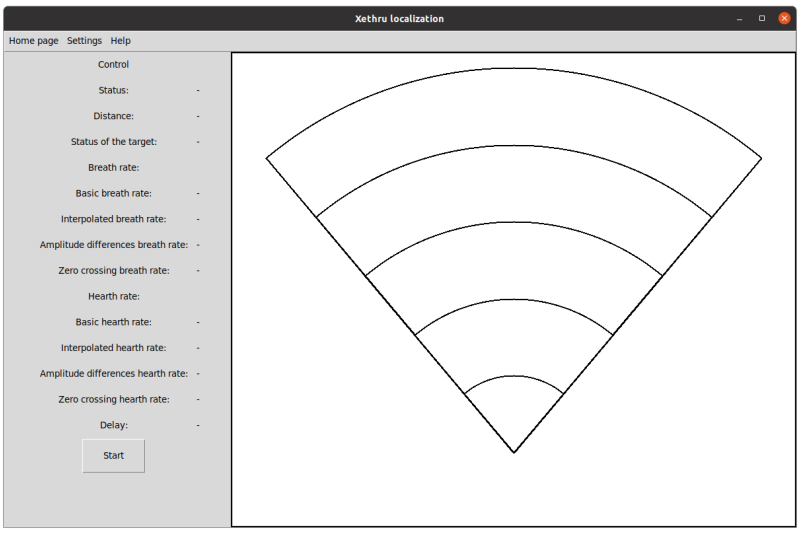

Figure 4.6: Graphical user interface.

[4]Tkinter library: https://docs.python.org/3/library/tkinter.html

4.2 Experiments

The solution was tested in operating system Linux Ubuntu 20.04 in the Python 3.5 with versions of the libraries: Matplotlib 3.0.3, NumPy 1.18.2, pymoduleConnector 1.6.2, pySerial 3.4, pyUSB 1.0.2 and SciPy 1.4.1. The communication library from Infineon has version 1.2.2. The evaluation was tested on the laptop with the RAM 16GB and the processor intel i5-8250U. There were tested only Xethru and Distance2GO radars because the Position2GO fell and was damaged.

4.2.1 Evaluation

Setup
The testing setup consists of two radars provided by the university, laptop, chest strap, phone and headphones with a microphone. Chest strap's model is Garmin HRM2-SS. This model is connected to the phone Samsung Galaxy S9+ via ANT+. On the phone, the application myWorkouts[5] shows the heart rate of the person. Since the respiratory rate makes a noise (inhalation and exhalation), the sound can be measured, and from the spectrum of the audio signal, the respiratory rate can be obtained. The microphone from the headphones is placed below the nose and is sensed via the Samsung's Recorder application. In the sensing process, the screen of the phone is split into two parts, and in each half of the screen, one sensing application runs. The display of the phone is cast by the application Screen Stream[6] which transports the screen via HTTP on the local network, and the phone's casted screen is opened in the laptop's browser. The radars are mounted on the microphone stand. Because the sensors need to be compared in the same situations, the evaluation applications for each radar are opened and run at the same time with the casted phone's screen to obtain reference values for the specific time. The video of the captured desktop window with desktop applications from both radars, casted screen from the phone and video of the room are recorded and saved for the future evaluation of the results 4.7. Each data frame was saved into the structure in the JSON file.

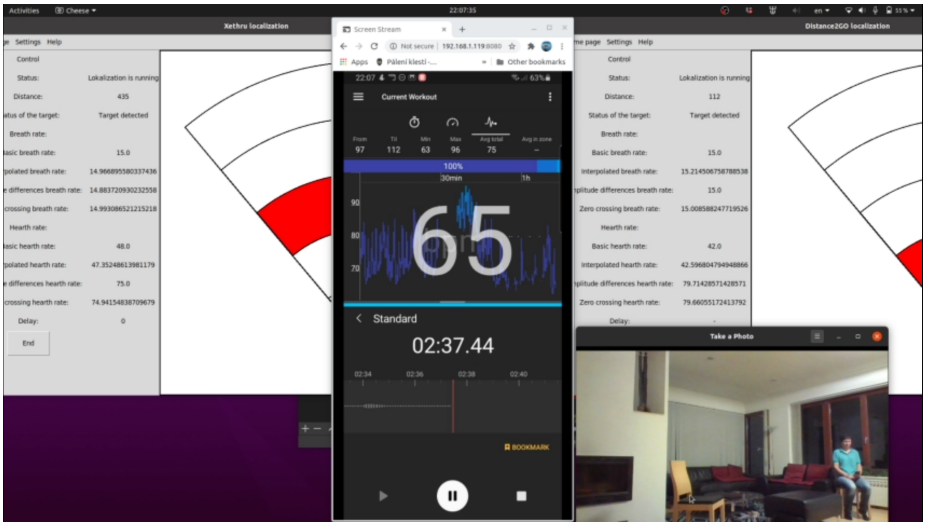

Figure 4.7: Recorded screen during the evaluation.

[5]myWorkouts: https://play.google.com/store/apps/details?id=org.myworkouts&hl=en
[6]Screen stream: https://play.google.com/store/apps/details?id=info.dvkr.screenstream&hl=en

Sensing and evaluation of the data

Three evaluation schemas were made to simulate the real situation of the usage of the radars, that means: sensing the person when it is motionless, recognize if the person is moving or not, or if there is no person at all. The person changes the respiratory rate once per one schema. The application, which is beeping based on the set period, helps to maintain the specific respiratory rate[7]. First evaluation schema took place in the smaller room 3,5x4,5m and the second one in the bigger room 5,5x6,3m. In the last schema, radars were sensing the person in the bed while it was sleeping.

In the small room, four evaluation places were placed on three spots, because at one spot, the person sat at two different angles. The tested person had to stay at each place for 80 seconds and in the half of the evaluation process, between the second and the third evaluation place, had to change the respiratory rate. While sitting in the second place, the person did small movements with the phone. Between the third and fourth place, the person was walking for a few seconds around the room. The person sat at a different angle to the radar in each place, and these spots were in these distances: 2.8, 2, 2.8, 3 m (in order of evaluation schema) 4.8.

Figure 4.8: The first evaluation room.

In the second schema, four evaluation places at three spots took place in the bigger room. The tested person had to stay at the first two evaluation places for 80 seconds and in the last two places for 60 seconds. The person had to change the respiratory rate between the second and the third evaluation place. The fourth evaluation place differs from the third one in the person sitting style, but it is placed at the same spot. The person sat back against the sofa compared to the third one, which caused worse sensing chest area for the radar. The person sat at a different angle to the radar in each place. These spots were in these distances: 3.1, 4.4, 6.2 meters 4.9.

The last evaluation schema consists of sensing and recording the person while sleeping in the bed during the night. The sensing distance is 1.60m 4.10.

Five people attended the process of testing, and all of them were tested five times on the first two schemas in each room. In the third schema, four people were evaluated each person once. The evaluation window was 20 seconds long and the evaluation was assessed every 20 seconds. Both values are a reasonable compromise between the accuracy and period of evaluated data. The Xethru radar sensing settings were set up to 5 meters in the smaller

[7]Breathe: https://play.google.com/store/apps/details?id=uk.co.jatra.inout&hl=en

Figure 4.9: The second evaluation room.

Figure 4.10: The third evaluation schema.

room and during the third schema and in the bigger room was set up to 8 meters. The Distance2GO radar is set for sensing up to 10 meters all the time.

The evaluation data saved in JSON were loaded via basic HTML page with JavaScript and JavaScript's library jQuery, which visualize the preview of the saved 20-second evaluation frames and the user chooses the frames, from which he counts the average values 4.11.

From the recorded video, the status mistakes are counted, e.g. the person is motionless, but the radar detects a person as a moving target. The frames in the evaluation page application are chosen based on the time from the recorded video while the person is sitting and breathing with the same respiratory rate. The heart rate is visually obtained from myWorkouts application. The respiratory rate are visually obtained from the spectrum of the recorder and from the application's period, which was beeping in the set period. The averages of the values of vital signs which are computed while the person is sitting on the given spots are counted during one measurement. From five measurements of one schema that are performed by one person, another average is obtained. In the next step of the evaluation, the average is counted from all measurements in one schema, regardless of the measured person. To compare the computing methods between themselves the averages of the first and second schema are counted and the best methods are selected.

The recorded video from the sleeping schema is too long for a detailed evaluation. That is why five random parts of the video were selected. Since the respiratory rate is

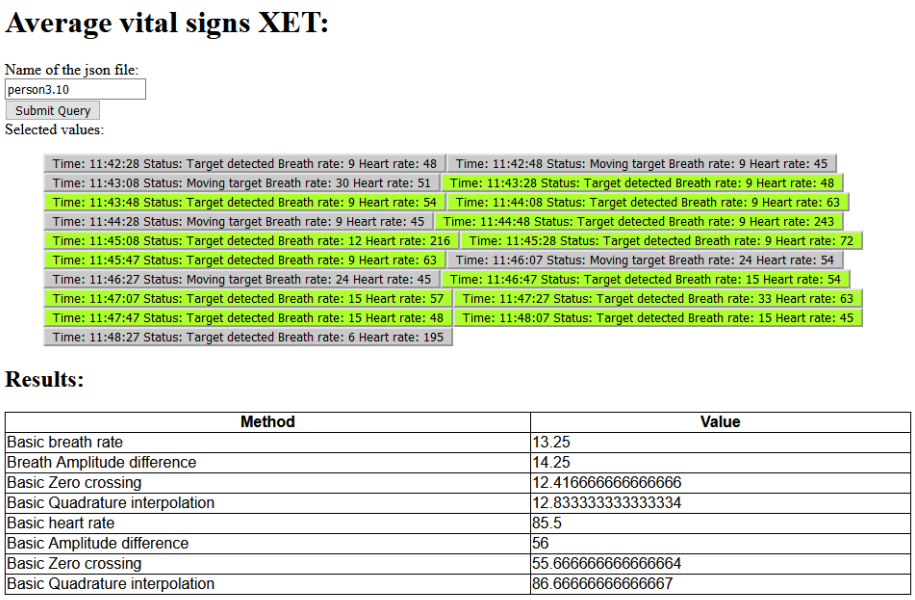

Figure 4.11: Helping evaluation application.

quite invariable during the sleep, the obtained respiratory rate values from the sound were selected and compared to the values from the video. The next evaluation part was checking if the radar is detecting the person all the time during the sleep and if the measured values make sense. The changes in the target status are quite easily visually detected in the video. Poorly detected parts were counted and the radar behavior was described.

4.2.2 Results

Data were evaluated according to the steps from the previous chapter 4.7.Even if the radars are sensing the space at the same time the testing process is not the same for both radars. Each radar has a different initialization period and that is why it runs in a different time and can have different evaluation time compared to the other radar. Especially when something happens at the early beginning or late end of the evaluation window, the radar can evaluate different situations compared to the other device. That is why reference values were counted individually for each radar. They were counted only for the correctly detected frames and that is the reason why they can differ from the average reference values of the other radar.

The status mistake was counted as each incorrect status of the radar. Status changes should appear with the new evaluation status. In extreme cases, changes should appear up to the time length of the evaluation window.

In the first schema, when the person manipulated the phone and the radar detected that the person was moving, it was considered as a mistake. In the second schema, when the person sat back (between the third and the fourth evaluation place) and radar detected the movement, it was considered as allowed behavior.

These two tables show the average values of each person of both radars for the specific schema. 4.12 4.13.

Eval. method/signal	XET1[8]	D2G1[9]	XET2	D2G2	XET3	D2G3	XET4	D2G4	XET5	D2G5
Ref.[10]res. r.[11]	13.79	14.00	12.63	12.68	12.44	11.62	12.46	12.43	12.47	12.85
Ref. hrt. r.[12]	72.60	72.60	68.20	68.20	65.80	65.80	56.00	56.00	79.00	79.00
Basic [13]res. r.	11.65	15.66	12.64	12.73	13.03	14.38	12.11	13.20	13.36	25.45
Diff. amplit.[14]res. r.	13.22	15.72	13.18	12.94	13.59	15.00	12.75	13.88	13.41	25.33
Zero cross.[15]res .r.	11.67	15.35	12.28	12.36	12.88	14.18	12.01	13.29	13.13	25.26
Quad. inter.[16]res. r.	11.01	14.87	11.99	11.59	12.38	14.13	11.70	12.08	12.87	25.46
Basic hrt. r.	63.44	58.64	58.83	62.06	62.94	63.55	56.85	58.11	52.23	67.13
Diff. amplit. hrt. r.	66.78	66.75	69.76	64.32	67.45	59.16	68.56	67.48	71.91	59.99
Zero cross. hrt. r.	66.93	66.38	65.94	64.06	67.39	58.72	68.80	67.25	71.97	59.66
Quad. inter. res. r.	62.82	59.26	58.24	61.49	62.29	62.37	56.13	56.65	51.65	68.83
False detection	0.80	5.80	1.20	4.20	1.00	9.00	0.20	5.80	0.80	9.00
Num. frames[17]	19.00	19.40	21.20	21.20	20.40	20.40	19.40	19.40	20.80	20.80

Figure 4.12: Average values of each person of the first schema.

Eval. method/signal	XET1	D2G1	XET2	D2G2	XET3	D2G3	XET4	D2G4	XET5	D2G5
Ref. res. r.	11.79	11.40	12.49	12.92	12.59	12.01	12.45	11.19	12.54	12.44
Ref. hrt. r.	75.20	75.20	76.20	76.20	66.00	66.00	62.20	62.20	72.00	72.00
Basic res. r.	12.64	13.42	12.96	14.94	12.07	13.92	14.79	15.97	13.34	19.45
Diff. amplit. res. r.	13.28	13.80	14.14	15.19	13.43	14.00	15.04	16.43	13.78	19.62
Zero cross. res. r.	12.64	13.27	12.69	14.88	12.11	13.72	14.55	16.03	12.94	19.17
Quad. inter. res. r.	12.16	11.07	12.45	13.66	11.53	12.95	14.31	14.72	12.82	18.06
Basic hrt. r.	78.79	61.72	64.47	55.63	77.15	56.23	62.63	54.59	71.28	56.95
Diff. amplit. hrt. r.	65.02	65.44	67.61	67.87	65.88	77.44	66.62	69.07	65.05	66.25
Zero cross. hrt. r.	65.10	65.14	67.68	67.65	65.99	77.06	66.39	68.98	64.77	65.88
Quad. inter. res. r.	78.21	61.29	64.15	55.24	76.62	55.17	62.03	54.06	70.63	56.47
False detection	0.20	0.80	0.00	4.20	0.20	4.40	0.20	5.60	0.00	4.00
Num. frames	17.40	17.60	19.40	19.40	18.00	18.60	17.80	17.80	18.80	19.00

Figure 4.13: Average values of each person of the second schema.

From these two tables can be observed, that radars achieved similar results from both schemas. The second schema was tested in a bigger and more open room. In the more open space, the signal did not reflect so much off the walls and that is why there was not so much noise. Compared to the second schema, the first one was in a smaller room, so there was a more noise, but the targets were closer. Both schemas contain some positions where the person was harder to detect, especially simulating some activity with the phone, sitting in a quite uncomfortable position on the bed, facing the radar from the side, sitting far from

[8] Xethru radar 1st person
[9] Distance 2 GO radar 1st person
[10] Ref. - Reference
[11] res. r. - Respiratory rate per minute
[12] hrt. r. - Heart rate per minute
[13] Basic - Basic FFT maximum peak method
[14] Diff. amplit. - Difference of the amplitude method
[15] Zero cross. - Zero crossing method
[16] Quad. inter. - Quadratic interpolation method
[17] Num. frames - Average number of evaluated frames

the radar under the poor angle. All these spots were causing none or strong nonperiodic signals and that is why sometimes the radar badly detect the vital signs.

Eval. method/signal	XET1[18]	D2G1[19]	XET2	D2G2	XET AVG	D2GO AVG
Ref. res. r.	12.76	12.72	12.37	11.99	12.57	12.35
Ref. hrt. r.	68.32	68.32	70.32	70.32	69.32	69.32
Basic res. r.	12.56	16.28	13.16	15.54	12.86	15.91
Diff. amplit. res. r.	13.23	16.57	13.94	15.81	13.58	16.19
Zero cross. res. r.	12.40	16.09	12.99	15.41	12.69	15.75
Quad. inter. res. r.	11.99	15.63	12.65	14.09	12.32	14.86
Basic hrt. r.	58.86	61.90	70.86	57.02	64.86	59.46
Diff. amplit. hrt. r.	68.89	63.54	66.04	69.21	67.46	66.38
Zero cross. hrt. r.	68.21	63.22	65.99	68.94	67.10	66.08
Quad. inter. res. r.	58.23	61.72	70.33	56.44	64.28	59.08
False detection	0.80	6.76	0.12	3.80	0.46	5.28
Num. frames	20.16	20.24	18.28	18.48	19.22	19.36

Table 4.1: Average values of both schemas and average of these averages.

In the last table 4.1 are presented averages of values from both schemas. The better solution is on the Xethru radar. The values are not so far among both radars, but in D2GO radar a lot of frames were not evaluated, because radar did not identify the person as motionless even though it was. That is why a lot of values were skipped and only the strong ones were evaluated. In the Xethru radar, less than 3% of target status were detected falsely.

The respiratory rate by the Xethru radar was reasonably detected in both schemas and by D2GO in some cases too. The heart rate from the table looks quite good too, but in a real situation, in the current time, the radar hit the correct value only sometimes. The best evaluation method for obtaining respiratory rate in Xethru radar based on the table was zero crossing and then quadratic interpolation. In D2GO it was Quadratic interpolation. The best evaluation methods for obtaining heart rate in both radars are amplitude differences of amplitudes and quadratic interpolation.

The Xethru radar worked in the third schema without any problems. The accuracy was +- 2-3 bpm and usually, results were exact. If the person turned in the bed or went out of the bed, the radar reacted on it correctly, it changed the status and when the person was motionless it began detecting vital signs. The D2GO radar did not detect the person during a sleep correctly. Most likely because of the mistake in the radar or communication library, after more than an hour this radar disconnected from the laptop.

Values from each test, from the first and second schema, can be found in the tables in appendix A. Video recordings with each person in each schema and all saved data in JSON file from the testing are attached on DVD B.

[18] Xethru radar 1st schema
[19] Distance 2 GO radar 1st schema

4.2.3 Sugestion for improvements

From time to time some of the results are not stable. It can be caused by not ideal monitoring angle between the radar and the target person, by the resolution of the radar or by small movements. To achieve better results, the more accurate radar or solution, which cooperates with more radars, is needed. Accuracy of radars is based on the bandwidth which is regulated with communication regulators and often there is not bandwidth long enough and that is why the special permission is needed. The solution based on more radar devices has not only a higher chance that the person is better faced to the radar but also can monitor several people. Radars can cover a bigger sensed space and cooperate together. The connection to all radars can be provided via remote communication with the server.

The better, more accurate radar usually obtains more data, and that is why to process this amount of data the faster algorithm will be needed. To speed up the solution, the algorithm can be implemented in c or c++ language, which is much faster than python.

These kinds of electronics are very sensitive and can be affected by external factors. Because these devices are cooled passively, the temperature can rise rapidly and the higher temperature can affect the sensed data. That is why the cooling system should be added to the final solution.

The last but very important suggestion is that it will be better to test this solution in a laboratory or with better reference devices. In laboratory settings, it is easier to control the undesirable extraneous variables which could affect the results. In this evaluation process can happen, that a little bit different values can be counted and the final result can be biased.

Chapter 5

Conclusion

Nowadays, in the era of smart solutions and a huge emphasis on data privacy, it is very desirable to detect the human presence anonymously and to recognize if the sensed person is in good health condition. This bachelor thesis aims to propose an algorithmic solution for the detection of people based on vital sign sensing, specifically on the heart and respiratory rate. After familiarization with the university provided radars, the solution is implemented. In the solution the data are sensed via UWB pulse radar or FMCW radar, then the signal is processed, vital signs are extracted and more precisely counted via additional methods. The thesis shows the functionality of the solution in the experimental measurements and presents their results.

The issues related to the topic of FMCW and UWB, radar signal processing and vital signs detection were studied in detail. Many articles, solutions and academic works were read to gain greater knowledge about the topic and explore possible ways how to implement the final solution.

As a part of the implementation, the Infineon's communication libraries were rewritten and connected to the python solution. Several filters, localization methods and other improvements for each radar were tried, and the final solution for each radar was created and except damaged position2GO also tested. For easier manipulation and measurements with the radar, the basic GUI was created, and the possibility to export sensed data into JSON file added.

The solution provides a real-time evaluation of the human for quite long distance, compared to other vital sign solution in this price category. The Xethru radar provides reasonable results which can detect if the human is moving, when the person is sufficiently facing the radar and detect him and his vital signs. This radar can also monitor person during sleep. Distance2GO radar provides not so pleasant results and that is primarily caused by the resolution of the radar which is only 0.75 m.

As a part of the evaluation two schemas, each in the different room, were created. In each schema, four spots in different distances and under different angles took places in the testing rooms. These two schemas were tested on five people and each person was tested five times in each schema. Four people were also tested during their sleep. All the values were evaluated and the methods were compared. This kind of research is still quite new, and the rapidly developing and affordable radar technologies provide many opportunities. Also because of the needs for the smart home's systems and restrictions from the data privacy, these technologies have huge potential.

There are many ways how to improve the detection of the people such as using more accurate radar devices, connecting more radars together and improve the processing algo-

rithm. That is the reason why it is definitely worth focusing on this topic and continue with onward research.

Bibliography

[1] Adib, F., Kabelac, Z., Katabi, D. and Miller, R. C. 3D Tracking via Body Radio Reflections. In: ACM. *Proceedings of the 11th USENIX Conference on Networked Systems Design and Implementation*. USA: USENIX Association, 2014, p. 317–329. NSDI'14. ISBN 9781931971096. Available at: https://www.usenix.org/conference/nsdi14/technical-sessions/presentation/adib.

[2] Adib, F., Mao, H., Kabelac, Z., Katabi, D. and Miller, R. C. Smart Homes That Monitor Breathing and Heart Rate. In: ACM. *Proceedings of the 33rd Annual ACM Conference on Human Factors in Computing Systems*. New York, NY, USA: Association for Computing Machinery, 2015, p. 837–846. CHI '15. DOI: 10.1145/2702123.2702200. ISBN 9781450331456.

[3] Al-Naji, A., Gibson, K., Lee, S. and Chahl, J. Monitoring of Cardiorespiratory Signal: Principles of Remote Measurements and Review of Methods. *IEEE Access*. IEEE. 2017, vol. 5, p. 15776–15790. DOI: 10.1109/ACCESS.2017.2735419.

[4] Álvarez Aparicio, C., Guerrero Higueras, Á. M., Rodríguez Lera, F. J., Olivera, M. C. C., Olivera, V. M. et al. LIDAR-based People Detection and Tracking for@ home Competitions. In: IEEE. *2019 IEEE International Conference on Autonomous Robot Systems and Competitions (ICARSC)*. 2019, p. 1–6. DOI: 10.1145/2702123.2702200. ISBN 978-1-7281-3558-8.

[5] Tutorials point. *Basic principle of radar* [online]. [cit. 2020-1-22]. Available at: https://www.tutorialspoint.com/radar_systems/radar_systems_overview.htm.

[6] *Detecting Heartbeats in Rubble* [online]. 2013 [cit. 2020-01-05]. Available at: https://www.dhs.gov/detecting-heartbeats-rubble-dhs-and-nasa-team-save-victims-disasters.

[7] Infineon. *Distance2Go* [online]. 2019 [cit. 2019-12-31]. Available at: https://www.infineon.com/cms/en/product/evaluation-boards/demo-distance2go/.

[8] Krynický, M. *Realisticky.cz* [online]. 2010 [cit. 2020-1-22]. Available at: http://www.realisticky.cz/ucebnice/02%20Fyzika%20S%C5%A0/03%20Kmitav%C3%BD%20pohyb%20a%20mechanick%C3%A9%20vln%C4%9Bn%C3%AD/03%20Zvukov%C3%A9%20vln%C4%9Bn%C3%AD/01%20%C5%A0%C3%AD%C5%99en%C3%AD%20zvuku,%20Doppler%C5%AFv%20efekt.pdf.

[9] Doran, D., Gokhale, S. and Dagnino, A. Human sensing for smart cities. In: ACM. *Proceedings of the 2013 IEEE/ACM International Conference on Advances in Social Networks Analysis and Mining*. 2013, p. 1323–1330. ISBN 9781450322409.

[10] Forbes, H. *Jarvis's Physical Examination and Health Assessment*. London: Elsevier Health Sciences APAC, 2011. ISBN 9780729579735.

[11] Hall, J. *Guyton and Hall textbook of medical physiology*. Philadelphia, PA: Saunders Elsevier, 2011. ISBN 9781437726749.

[12] Homolka, P. *Monitorovani krevniho tlaku v klinicke praxi a biologicke rytmy*. 1st ed. Praha: Grada, 2010. ISBN 978-80-247-2896-4.

[13] *How Infrared motion detector components work* [online]. 2015 [cit. 2020-01-05]. Available at: http://www.glolab.com/pirparts/infrared.html.

[14] Infineon. *Frequently asked questions for 24 GHz industrial radar* [online]. 10. 2018. Available at: https://www.infineon.com/dgdl/Infineon-Radar%20FAQ-PI-v02_00-EN.pdf?fileId=5546d46266f85d6301671c76d2a00614.

[15] Infineon. *Position2Go software user manual* [online]. 39. 2019. Available at: https://www.infineon.com/dgdl/Infineon-P2G_Software_User_Manual-ApplicationNotes-v01_01-EN.pdf?fileId=5546d4626b2d8e69016b89493bf842afl.

[16] Infineon. *Position2Go software user manual* [online]. V1.1th ed. 2019. Available at: https://www.infineon.com/dgdl/Infineon-P2G_Software_User_Manual-ApplicationNotes-v01_01-EN.pdf?fileId=5546d4626b2d8e69016b89493bf842af.

[17] *IMS Band Frequencies* [online]. [cit. 2020-01-05]. Available at: https://www.itu.int/net/ITU-R/terrestrial/faq/index.html#g013.

[18] Ivašić Kos, M., Krišto, M. and Pobar, M. Human Detection in Thermal Imaging Using YOLO. In: ICCTA, ed. *Proceedings of the 2019 5th International Conference on Computer and Technology Applications*. Association for Computing Machinery, April 2019, p. 20–24. DOI: 10.1145/3323933.3324076. ISBN 9781450371810.

[19] Jardak, S., Kiuru, T., Metso, M., Pursula, P., Häkli, J. et al. Detection and localization of multiple short range targets using FMCW radar signal. In: IEEE. *2016 Global Symposium on Millimeter Waves (GSMM) ESA Workshop on Millimetre-Wave Technology and Applications*. 2016, p. 1–4. ISBN 978-1-5090-1348-7.

[20] Kebe, M., Gadhafi, R., Mohammad, B., Sanduleanu, M., Saleh, H. et al. Human Vital Signs Detection Methods and Potential Using Radars: A Review. *Sensors*. MDPI AG. Mar 2020, vol. 20, no. 5, p. 1454. DOI: 10.3390/s20051454. ISSN 1424-8220. Available at: http://dx.doi.org/10.3390/s20051454.

[21] Levanon, N. *Radar signals*. Hoboken: John Wiley & Sons, 2004. ISBN 0-471-47378-2.

[22] Luděk, D. *Radarové měření vzdálenosti* [online]. Plzeň, 2012. Bachelor's thesis. Západočeská univerzita v Plzni. Fakulta elektrotechnická.

[23] Lyons, R. Quadrature Signals: Complex, But Not Complicated. IEEE. 2008. Available at: https://www.ieee.li/pdf/essay/quadrature_signals.pdf.

[24] Morbiducci, U., Scalise, L., Melis, M. and Grigioni, M. Optical Vibrocardiography: A Novel Tool for the Optical Monitoring of Cardiac Activity. *Annals of biomedical engineering*. november 2007, vol. 35, no. 1, p. 45–58. DOI: 10.1007/s10439-006-9202-9.

[25] Novelda AS. *XeThru X4 Phase Noise Correction*. 13, Rev. Ath ed. 2018. Available at: https://github.com/novelda/Legacy-Documentation/blob/master/Application-Notes/XTAN-14_XeThru_X4_Phase_Noise_Correction_rev_a.pdf.

[26] Novelda AS. *XeThru X4 Radar User Guide* [online]. Rev. Ath ed. 2018. Available at: https://github.com/novelda/Legacy-Documentation/blob/master/Application-Notes/XTAN-13_XeThruX4RadarUserGuide_rev_a.pdf.

[27] Infineon. *Position2Go* [online]. 2019 [cit. 2019-12-31]. Available at: https://www.infineon.com/cms/en/product/evaluation-boards/demo-position2go/.

[28] Sapra, A., Malik, A. and Bhandari, P. Vital Sign Assessment. In: *StatPearls [Internet]*. StatPearls Publishing, 2019. Available at: https://www.ncbi.nlm.nih.gov/books/NBK553213/#_NBK553213_pubdet_.

[29] Skolnik, M. I. M. I. *Introduction to radar systems*. 3rd ed.th ed. Boston: McGraw-Hill, 2001. MCGraw-Hill higher education. ISBN 978-0-07-288138-7.

[30] Smith, J., Music, S. U. C. for Computer Research in, Acoustics and Music, S. U. D. of. *Spectral Audio Signal Processing*. W3K, 2011. ISBN 9780974560731. Available at: https://ccrma.stanford.edu/~jos/sasp/.

[31] Tse, D. and Viswanath, P. *Fundamentals of Wireless Communication*. USA: Cambridge University Press, 2005. ISBN 0521845270.

[32] Vrba, J. *Úvod do mikrovlnné techniky*. 2. přeprac. vyd.th ed. Praha: ČVUT, 2007. ISBN 978-80-01-03670-9.

[33] Wang, G., Gu, C., Inoue, T. and Li, C. A hybrid FMCW-interferometry radar for indoor precise positioning and versatile life activity monitoring. *IEEE Transactions on Microwave Theory and Techniques*. IEEE. november 2014, vol. 62, no. 11, p. 2812–2822. ISSN 0018-9480.

[34] Novelda AS. *X4M03* [online]. 2019 [cit. 2019-12-31]. Available at: https://www.xethru.com/xethru-development-platform.html.

Appendix A

Detail results from testing

Tables with detail values from the testing

Eval. met./sig.	XET1[1]	D2G1[2]	XET2	D2G2	XET3	D2G3	XET4	D2G4	XET5	D2G5
Ref.[3]res. r.[4]	11.81	11.82	11.82	11.67	12.50	12.22	10.91	11.79	21.92	22.50
Ref. hrt. r.[5]	75.00	75.00	74.00	74.00	72.00	72.00	71.00	71.00	71.00	71.00
Basic[6]res. r.	10.91	17.73	10.91	13.25	10.50	10.00	9.55	16.71	16.38	20.63
Diff. amplit.[7]res. r.	13.45	17.27	10.82	13.25	13.08	10.67	9.45	16.43	19.31	21.00
Zero cross.[8]res. r.	10.82	17.36	10.45	12.83	10.75	10.33	9.27	15.86	17.08	20.38
Quad. inter.[9]res. r.	10.27	17.09	10.45	12.17	9.92	8.56	8.73	16.43	15.69	20.13
Basic hrt. r.	52.09	66.82	85.64	56.50	68.00	70.00	55.64	48.86	55.85	51.00
Diff. amplit. hrt. r.	70.73	60.91	64.09	69.25	60.08	58.78	73.91	73.43	65.08	71.38
Zero cross. hrt. r.	70.64	60.55	64.73	69.50	59.42	58.44	74.55	72.29	65.31	71.13
Quad. inter. hrt. r.	51.36	72.45	85.18	55.50	67.33	69.33	54.82	49.14	55.38	49.88
False detection	2.00	6.00	2.00	5.00	0.00	6.00	0.00	6.00	0.00	6.00
Num. frames[10]	19.00	19.00	20.00	20.00	19.00	19.00	18.00	19.00	19.00	20.00

Figure A.1: Detail values of the first person in the first schema.

[1] Xethru radar 1st repetition
[2] Distance 2 GO radar 1st repetition
[3] Ref. - Reference
[4] res. r. - Respiratory rate per minute
[5] hrt. r. - Heart rate per minute
[6] Basic - Basic FFT maximum peak method
[7] Diff. amplit. - Difference of the amplitude method
[8] Zero cross. - Zero crossing method
[9] Quad. inter. - Quadratic interpolation method
[10] Num. frames - Average number of evaluated frames

Eval. met./sig.	XET6	D2G6	XET7	D2G7	XET8	D2G8	XET9	D2G9	XET10	D2G10
Ref. res. r.	12.08	11.50	12.08	11.54	12.73	12.31	13.18	12.73	8.86	8.93
Ref. hrt. r.	74.00	74.00	74.00	74.00	77.00	77.00	76.00	76.00	75.00	75.00
Basic res. r.	11.50	13.75	16.25	12.69	13.36	12.92	13.36	16.36	8.73	11.36
Diff. amplit. res. r.	13.08	14.17	18.25	13.62	13.45	13.23	12.82	16.36	8.82	11.64
Zero cross. res. r.	11.83	13.67	16.83	12.69	13.09	12.46	12.73	16.18	8.73	11.36
Quad. inter. res. r.	11.33	9.00	16.00	13.31	12.91	12.00	12.45	15.82	8.09	5.21
Basic hrt. r.	62.75	64.00	55.75	60.92	146.18	63.69	49.64	61.91	79.64	58.07
Diff. amplit. hrt. r.	65.17	64.58	67.50	66.92	55.09	63.31	73.18	64.91	64.18	67.50
Zero cross. hrt. r.	64.67	64.08	68.08	66.92	54.91	62.77	73.73	64.64	64.09	67.29
Quad. inter. hrt. r.	62.50	64.83	54.83	60.08	145.73	62.92	49.09	61.18	78.91	57.43
False detection	0.00	2.00	0.00	0.00	1.00	0.00	0.00	2.00	0.00	0.00
Num. frames	17.00	17.00	17.00	18.00	18.00	17.00	17.00	18.00	18.00	18.00

Figure A.2: Detail values of the first person in the second schema.

Eval. met./sig.	XET1	D2G1	XET2	D2G2	XET3	D2G3	XET4	D2G4	XET5	D2G5
Ref. res. r.	12.78	12.73	12.69	11.88	12.67	13.75	12.50	12.31	12.50	12.73
Ref. hrt. r.	71.00	71.00	68.00	68.00	67.00	67.00	69.00	69.00	66.00	66.00
Basic res. r.	12.67	12.55	12.92	13.50	12.80	11.50	11.75	12.46	13.07	13.64
Diff. amplit. res. r.	13.00	12.36	13.38	13.19	14.33	12.33	11.33	12.92	13.86	13.91
Zero cross. res. r.	12.89	12.27	11.92	13.25	12.53	11.17	11.42	11.85	12.64	13.27
Quad. inter. res. r.	12.00	11.91	12.15	12.19	12.20	11.17	11.00	10.23	12.57	12.45
Basic hrt. r.	48.33	60.82	59.77	66.94	71.33	75.50	51.50	53.31	63.21	53.73
Diff. amplit. hrt. r.	73.78	66.73	65.85	63.06	71.60	52.17	71.08	70.54	66.50	69.09
Zero cross. hrt. r.	74.11	66.64	65.92	63.13	51.47	52.00	71.92	70.08	66.29	68.45
Quad. inter. hrt. r.	48.00	60.18	59.00	66.19	70.65	75.00	50.83	52.69	62.71	53.36
False detection	5.00	6.00	0.00	2.00	0.00	8.00	1.00	1.00	0.00	4.00
Num. frames	22.00	22.00	20.00	20.00	24.00	24.00	20.00	20.00	20.00	20.00

Figure A.3: Detail values of the second person in the first schema.

Eval. met./sig.	XET6	D2G6	XET7	D2G7	XET8	D2G8	XET9	D2G9	XET10	D2G10
Ref. res. r.	12.31	13.00	12.92	12.69	12.31	12.73	12.86	13.33	12.08	12.86
Ref. hrt. r.	78.00	78.00	79.00	79.00	77.00	77.00	75.00	75.00	72.00	72.00
Basic res. r.	12.92	15.30	11.75	15.92	13.15	15.00	13.71	14.33	13.25	14.14
Diff. amplit. res. r.	13.54	15.10	12.08	16.15	14.85	16.36	16.00	14.78	14.25	13.57
Zero cross. res. r.	13.08	15.80	11.33	15.69	12.85	14.64	13.79	14.56	12.42	13.71
Quad. inter. res. r.	12.69	14.50	11.25	14.15	12.54	14.09	12.93	13.11	12.83	12.43
Basic hrt. r.	48.00	54.90	50.00	51.46	83.77	54.27	55.07	59.67	85.50	57.86
Diff. amplit. hrt. r.	76.23	66.60	73.75	71.77	63.92	68.27	68.14	67.00	56.00	65.71
Zero cross. hrt. r.	76.77	66.70	73.42	71.54	63.85	68.18	68.71	66.56	55.67	65.29
Quad. inter. hrt. r.	47.31	54.40	49.50	51.54	82.85	53.64	54.43	58.89	86.67	57.71
False detection	0.00	5.00	0.00	2.00	0.00	3.00	0.00	5.00	0.00	6.00
Num. frames	19.00	19.00	18.00	18.00	20.00	20.00	20.00	20.00	20.00	20.00

Figure A.4: Detail values of the second person in second schema.

Eval. met./sig.	XET1	D2G1	XET2	D2G2	XET3	D2G3	XET4	D2G4	XET5	D2G5
Ref. res. r.	11.92	11.11	12.69	12.00	12.08	12.50	13.00	10.00	12.50	12.50
Ref. hrt. r.	56.00	56.00	65.00	65.00	71.00	71.00	72.00	72.00	65.00	65.00
Basic res. r.	13.38	17.00	15.86	8.40	11.50	13.50	12.00	16.50	12.43	16.50
Diff. amplit. res. r.	14.15	17.78	16.21	11.20	12.00	13.50	12.20	16.50	13.36	16.00
Zero cross. res. r.	13.31	16.67	15.86	8.40	11.17	13.33	12.00	16.50	12.07	16.00
Quad. inter. res. r.	12.85	16.67	15.21	8.00	10.83	13.00	11.30	15.00	11.71	18.00
Basic hrt. r.	51.00	54.67	49.29	72.60	53.00	58.50	83.40	63.00	78.00	69.00
Diff. amplit. hrt. r.	71.85	70.22	75.14	51.60	69.58	63.50	58.30	57.50	62.36	53.00
Zero cross. hrt. r.	71.62	70.22	75.14	50.40	69.67	63.00	58.40	57.00	62.14	53.00
Quad. inter. hrt. r.	50.08	53.56	48.64	71.80	52.58	58.00	82.70	60.50	77.43	68.00
False detection	3.00	6.00	0.00	9.00	1.00	9.00	1.00	8.00	0.00	13.00
Num. frames	23.00	23.00	20.00	20.00	20.00	20.00	19.00	19.00	20.00	20.00

Figure A.5: Detail values of the third person in first schema.

Eval. met./sig.	XET6	D2G6	XET7	D2G7	XET8	D2G8	XET9	D2G9	XET10	D2G10
Ref. res. r.	12.92	13.33	12.86	11.67	13.18	13.57	12.08	11.00	11.92	10.50
Ref. hrt. r.	64.00	64.00	67.00	67.00	68.00	68.00	66.00	66.00	65.00	65.00
Basic res. r.	11.75	16.67	12.21	17.00	12.00	10.71	14.00	13.20	10.38	12.00
Diff. amplit. res. r.	12.58	16.22	12.64	17.89	13.64	10.57	15.92	13.60	12.38	11.70
Zero cross. res. r.	12.00	16.33	12.43	17.00	12.00	10.14	13.67	13.40	10.46	11.70
Quad. inter. res. r.	11.08	16.00	11.86	16.44	11.18	10.00	13.67	11.20	9.85	11.10
Basic hrt. r.	59.75	59.33	78.43	47.00	78.27	55.71	92.00	65.40	77.31	53.70
Diff. amplit. hrt. r.	68.58	67.00	68.57	76.67	63.00	65.86	62.33	108.80	66.92	68.90
Zero cross. hrt. r.	68.25	66.89	68.79	76.11	62.91	65.00	62.00	108.60	68.00	68.70
Quad. inter. hrt. r.	59.00	58.89	77.93	45.22	77.91	54.71	91.58	64.00	76.69	53.00
False detection	0.00	3.00	0.00	5.00	0.00	3.00	1.00	7.00	0.00	4.00
Num. frames	19.00	20.00	18.00	18.00	17.00	18.00	18.00	19.00	18.00	18.00

Figure A.6: Detail values of the third person in second schema.

Eval. met./sig.	XET1	D2G1	XET2	D2G2	XET3	D2G3	XET4	D2G4	XET5	D2G5
Ref. res. r.	12.50	12.78	12.69	12.73	12.33	11.67	12.50	12.50	12.27	12.50
Ref. hrt. r.	56.00	56.00	55.00	55.00	56.00	56.00	55.00	55.00	58.00	58.00
Basic res. r.	14.36	11.33	10.38	13.91	12.40	15.75	9.75	10.50	13.64	14.50
Diff. amplit. res. r.	14.71	13.56	11.77	14.82	12.20	15.83	11.33	10.38	13.73	14.83
Zero cross. res. r.	14.21	12.11	10.69	14.91	11.87	15.67	9.92	9.75	13.36	14.00
Quad. inter. res. r.	14.00	10.89	10.15	13.64	11.73	14.08	9.33	8.13	13.27	13.67
Basic hrt. r.	52.07	55.33	54.69	56.73	67.20	54.00	49.75	55.50	60.55	69.00
Diff. amplit. hrt. r.	71.64	68.22	69.46	71.36	66.40	69.58	72.58	65.25	62.73	63.00
Zero cross. hrt. r.	71.93	67.11	69.54	71.27	66.27	70.08	73.33	65.13	62.91	62.67
Quad. inter. hrt. r.	51.21	54.22	54.08	55.91	66.47	50.67	49.00	54.13	59.91	68.33
False detection	0.00	6.00	0.00	5.00	0.00	6.00	1.00	5.00	0.00	7.00
Num. frames	20.00	20.00	19.00	19.00	19.00	19.00	20.00	20.00	19.00	19.00

Figure A.7: Detail values of the fourth person in first schema.

Eval. met./sig.	XET6	D2G6	XET7	D2G7	XET8	D2G8	XET9	D2G9	XET10	D2G10
Ref. res. r.	13.00	10.00	12.27	11.25	12.92	12.50	13.40	14.50	11.60	11.00
Ref. hrt. r.	63.00	63.00	64.00	64.00	60.00	60.00	59.00	59.00	65.00	65.00
Basic res. r.	16.91	15.00	15.00	9.75	15.25	23.00	14.06	18.90	12.75	13.20
Diff. amplit. res. r.	17.45	15.00	14.82	10.13	15.42	22.92	14.44	19.70	13.08	14.40
Zero cross. res. r.	16.91	15.00	14.27	10.25	14.83	22.42	14.06	18.90	12.67	13.60
Quad. inter. res. r.	16.27	14.50	14.36	8.38	14.92	21.00	13.69	17.90	12.33	11.80
Basic hrt. r.	55.09	43.50	88.36	56.63	60.25	58.50	54.94	59.70	54.50	54.60
Diff. amplit. hrt. r.	67.55	82.50	63.82	67.63	63.75	65.00	68.00	63.20	70.00	67.00
Zero cross. hrt. r.	67.73	82.50	63.09	67.50	63.67	64.50	67.63	63.20	69.83	67.20
Quad. inter. hrt. r.	54.36	43.50	87.82	55.50	59.83	59.50	54.13	58.00	54.00	53.80
False detection	0.00	8.00	0.00	5.00	0.00	2.00	0.00	6.00	1.00	7.00
Num. frames	16.00	15.00	18.00	18.00	18.00	18.00	20.00	20.00	17.00	18.00

Figure A.8: Detail values of the fourth person in second schema.

Eval. met./sig.	XET1	D2G1	XET2	D2G2	XET3	D2G3	XET4	D2G4	XET5	D2G5
Ref. res. r.	12.86	13.57	12.50	13.00	12.67	11.43	12.67	15.00	11.67	11.25
Ref. hrt. r.	80.00	80.00	83.00	83.00	78.00	78.00	80.00	80.00	74.00	74.00
Basic res. r.	11.36	22.71	13.50	16.80	13.60	30.00	14.60	30.00	13.75	27.75
Diff. amplit. res. r.	11.79	22.57	13.88	16.60	13.47	29.71	14.27	30.00	13.67	27.75
Zero cross. res. r.	11.71	22.86	13.00	16.20	13.33	30.00	14.20	30.00	13.42	27.25
Quad. inter. res. r.	10.79	21.71	13.13	15.00	13.20	29.14	14.00	29.43	13.25	32.00
Basic hrt. r.	58.50	55.29	51.56	70.80	52.20	60.43	48.40	68.14	50.50	81.00
Diff. amplit. hrt. r.	67.64	66.86	72.13	59.60	72.27	63.43	74.67	58.57	72.83	51.50
Zero cross. hrt. r.	68.07	65.71	71.63	59.20	72.40	63.29	74.67	58.86	73.08	51.25
Quad. inter. hrt. r.	57.79	66.71	50.81	70.20	51.67	59.43	47.73	67.57	50.25	80.25
False detection	0.00	8.00	0.00	10.00	2.00	8.00	0.00	8.00	2.00	11.00
Num. frames	20.00	20.00	22.00	22.00	22.00	22.00	20.00	20.00	20.00	20.00

Figure A.9: Detail values of the fifth person in first schema.

Eval. met./sig.	XET6	D2G6	XET7	D2G7	XET8	D2G8	XET9	D2G9	XET10	D2G10
Ref. res. r.	12.33	12.50	12.67	12.08	12.50	12.69	12.33	12.08	12.86	12.86
Ref. hrt. r.	73.00	73.00	75.00	75.00	75.00	75.00	72.00	72.00	65.00	65.00
Basic res. r.	14.00	21.00	12.00	14.50	10.50	25.62	15.40	16.00	14.79	20.14
Diff. amplit. res. r.	13.87	22.38	13.13	14.92	10.81	25.31	16.07	15.50	15.00	20.00
Zero cross. res. r.	13.67	21.00	11.53	14.17	9.94	25.23	14.87	15.58	14.71	19.86
Quad. inter. res. r.	13.47	18.50	11.60	13.33	10.00	23.92	14.80	15.42	14.21	19.14
Basic hrt. r.	60.80	57.38	51.20	65.25	80.81	53.77	64.60	56.50	99.00	51.86
Diff. amplit. hrt. r.	65.60	65.25	72.00	59.42	64.56	69.54	63.87	66.75	59.21	70.29
Zero cross. hrt. r.	65.13	64.75	71.93	59.33	64.31	68.92	63.40	66.83	59.07	69.57
Quad. inter. hrt. r.	60.20	56.50	50.60	63.75	80.13	55.08	63.67	55.58	98.57	51.43
False detection	0.00	6.00	0.00	5.00	0.00	2.00	0.00	1.00	0.00	6.00
Num. frames	19.00	20.00	18.00	18.00	18.00	18.00	21.00	21.00	18.00	18.00

Figure A.10: Detail values of the fifth person in second schema.

Appendix B

DVD Structure

Structure of the attached DVD's files is:

- **/program/D2GO** Program for D2GO radar with library.
- **/program/P2GO** Program for P2GO radar with library.
- **/program/xethru** Program for xethru radar.
- **/README.md** Description of DVD structure and how to run the program.
- **/sources** Important sources for this thesis (communication libraries, documentations, manuals, etc.).
- **/tests/JSON** Folder with helping evaluation script and folders with obtained data from the testing.
- **/tests/video** Part of the video recordings from the radar testing.
- **/text** The thesis latex project with Makefile and BibTeX.
- **/xplace01.pdf** Text of the thesis.